Review

Bioprocess membrane technology

Robert van Reis [*], Andrew Zydney

Genentech, Inc., 1 DNA Way, South San Francisco, CA 94080, United States

Abstract

Membrane processes play a critical role in the purification of biotechnology products. Early membrane systems were adopted from technology originally developed for other industrial applications. During the last 2 decades, new membranes and modules have been developed specifically to meet the requirements of the biotechnology industry. This includes applications of membranes for sterile filtration, clarification, initial harvest, virus removal, protein concentration, buffer exchange, and protein purification. This manuscript provides an overview of recent developments in membrane technology, focusing on the special characteristics of the membrane systems that are now used for the commercial production and purification of recombinant protein products. Future developments in membrane technology are also discussed that may be able to meet the growing needs for higher productivity, lower cost of production, and increased development speed in the biotechnology industry.
© 2007 Elsevier B.V. All rights reserved.

Keywords: Biotechnology; Recombinant DNA; Protein; Microfiltration; Ultrafiltration

Contents

* Corresponding author. Tel.: +1 650 225 1522; fax: +1 650 225 4049.
  E-mail address: rvr@gene.com (R. van Reis).

1. Introduction—membrane applications overview

Membrane processes have been used for bioseparations since well before the start of the modern membrane industry. For example, John D. Ferry's review article on ultrafiltration in 1936 [1] described the use of membrane technology for enzyme concentration, analysis of bacteriophages and viruses, preparation of cell- and protein-free ultrafiltrates from biological solutions, and sterile filtration, although these systems were limited to analytical-scale processes due to limitations on the available membranes and modules.

Membrane systems also played a major role in the purification of the earliest biotechnology products [2,3], with these processes adopted directly from technology that was originally developed for the blood fractionation, food, dairy, and water industries [4]. Over the last 2 decades, new membranes, modules, and systems have been developed specifically to meet the requirements of the biotechnology industry. The objective of this review is to provide an overview of these developments, focusing on the special characteristics of the membrane systems that are now used in the production and purification of recombinant protein products.

1.1. Definitions of membrane processes

Although essentially all membrane processes are used for bioseparations, the greatest interest has been in the application of the pressure-driven processes of ultrafiltration, microfiltration, and virus filtration (Fig. 1). Reverse osmosis is also used extensively in the production of high quality water (WFI = water for injection), but the design of reverse osmosis systems is outside the scope of this review. Ultrafiltration membranes have pore sizes between 1 and 20 nm and are designed to provide high retention of proteins and other macromolecules (Section 8). Ultrafiltration membranes can also be used for protein purification using a process known as high performance tangential flow filtration (HPTFF, Section 9). Microfiltration membranes have pore size between 0.05 and 10 μm and are designed to retain cells and cell debris while allowing proteins and smaller solutes to pass into the filtrate (Sections 3 and 4). Membranes designed specifically for virus filtration fall between these limits and have pore size between 20 and 70 nm (Section 5). Virus filtration membranes are occasionally (but incorrectly) referred to in the literature as nanofiltration membranes based on their 20–70 nanometer pore size. Nanofiltration is properly defined as a process that separates solvent, monovalent salts, and small organics from divalent ions and larger species (Fig. 1). Depth filters are not typically considered as membranes since they retain key components throughout the porous structure. Removal rates are determined by both adsorptive and size-based retention mechanisms.

Normal flow filtration, also referred to as direct flow or dead-end filtration, is used primarily for systems in which the

Fig. 1. Comparison of removal characteristics of different pressure-driven membrane processes.

retained components are present at very low concentration. Normal flow is also used in depth filtration and membrane chromatography where the removal occurs throughout the porous structure. Large-scale ultrafiltration devices use tangential flow filtration in which the feed flow is directed parallel to the membrane and thus perpendicular to the filtrate flow [5,6]. This allows retained species to be swept along the membrane surface and out of the device, significantly increasing the process flux compared to that obtained in normal flow filtration.

In addition to the membrane processes used in the biotechnology industry, membrane technology has also played a major role in biomedicine. Hemodialysis, which is used to treat chronic kidney failure, is the single largest market for membranes with current usage in excess of $50 \times 10^6 \, \mathrm{m}^2$ of membrane per year. Solute removal in hemodialysis is primarily by diffusion, in sharp contrast to the convective transport that dominates the pressure-driven membrane processes. Membrane plasmapheresis, which is used extensively for both plasma collection and for the therapeutic removal of circulating pathogens from blood, is very closely related to tangential flow microfiltration.

1.2. Key membrane phenomena

Membranes are typically described by their pore size or nominal molecular weight cut-off (MWCO), with the latter typically defined as the molecular weight of a solute that has a retention coefficient of 90%. However, the key characteristics in the design of a membrane process are really the selectivity, the volumetric flux, and the system capacity. The intrinsic selectivity of the membrane is determined by the underlying pore size distribution and the membrane surface properties. For example, highly selective ultrafiltration membranes can be developed using electrically charged membranes that have very high retention of proteins with the same polarity [7,8]. Similarly, adsorptive membranes can provide highly selective separations based on the specific binding of various components. For pressure-driven membrane processes, the selectivity is directly related to the solute sieving coefficient:

$$S = \frac{C_f}{C_F} \tag{1}$$

where C_f and C_F are the solute concentrations in the filtrate and feed solutions, respectively.

The initial volumetric filtrate flux is related to the membrane hydraulic permeability:

$$L_p = \frac{J}{\Delta P} \tag{2}$$

where J is the filtrate flux (volumetric flow rate per unit membrane area) and ΔP is the transmembrane pressure difference. The filtrate flux evaluated using the actual feedstock of interest is typically less than the value predicted from the clean membrane permeability due to fouling and concentration polarization effects [6]. Membrane fouling can arise from adsorption on and within the membrane pores and/or from the formation of a deposit on the external surface of the membrane. Concentration polarization refers to the accumulation of completely or partially retained solutes at the upstream surface of the membrane due to bulk mass transfer limitations in the membrane device. In the case of microfiltration, the increased concentration of cells and cell debris can reduce the filtrate flux by providing an additional hydraulic resistance to flow. The dominant effect in protein ultrafiltration is the reduction in the effective pressure driving force due to osmotic pressure effects [9]. The extent of concentration polarization can be controlled by adjusting the fluid flow characteristics, typically by providing high local shear rates in tangential flow filtration modules or by inducing secondary flow involving Taylor [10] or Dean [11] vortices.

The system capacity is defined as the volume of feed that can be processed per unit membrane area before the membrane must be regenerated or replaced. For pressure-driven membrane processes operated at a constant transmembrane pressure, the capacity is typically defined as the point at which the filtrate flow rate has dropped to less than 10% of its initial value or below a pre-determined flux that is required for the particular application. For operation at constant filtrate flux, the capacity is defined by the maximum pressure drop that can be tolerated by the system. This might be limited by the membrane, the housing,

or a series of pressure drops that lead to a limitation on some other piece of equipment such as an upstream chromatography column. The capacity of an adsorptive membrane is defined by the appearance of an unacceptable level of a key component in the flow-through stream (referred to as breakthrough). Breakthrough is determined by both the equilibrium (static) binding properties of the resin in combination with any mass transfer limitations in the device. The capacity of depth filters can be determined by either breakthrough of a key component or by an unacceptable pressure drop, whichever occurs first under the actual process conditions.

2. Overview of bioprocessing

2.1. Properties of biomolecules

The early biotechnology products were highly active hormones (e.g., insulin, human growth hormone, erythropoietin), thrombolytic agents (e.g., tissue-type plasminogen activator), and clotting factors (e.g., Factor VIII). These proteins have unique biocatalyst activity, initiating or inhibiting complex biological cascades that give rise to the desired physiologic response. In contrast, many of the recent product introductions are monoclonal antibodies used for the treatment of breast cancer (Herceptin®), B-cell lymphoma (Rituxan®), and rheumatoid arthritis (Remicade® and Enbrel®), among others [12]. These molecules act stoichiometrically, binding to a particular receptor or cell type, requiring much higher dosing levels and batch sizes. Current annual production requirements are around 1000 kg, which are 100–1000-fold higher than the typical requirements for most of the early recombinant protein products.

The biological activity of a protein is determined by its unique three-dimensional structure and surface functionality. Proteins are biopolymers formed by a linear sequence of the 20 natural-occurring amino acids. The native state (or conformation) is stabilized primarily by hydrophobic interactions due to the unfavorable free energy associated with solvation of non-polar groups by water. The net result is that the non-polar side chains tend to collapse together to form the protein's hydrophobic core. Hydrogen bonds between weak acid donor groups (e.g., N–H and O–H) and acceptor groups with lone pair electrons stabilize the protein's secondary structure including both α-helices and β-sheets. Positively-charged amino groups and negatively-charged carboxylic acid groups are typically located along the protein exterior [13]. The net protein charge is determined by the number and pK_a of these acidic and basic amino acids. The isoelectric point (pI) is the pH at which the protein has no net electrical charge, typically determined by the equilibrium position in an isoelectric focusing gel or the lack of motion in an applied electric field.

Since the three-dimensional geometry of a given protein can be quite complex, the hard sphere radius is usually estimated from the measured diffusion coefficient using the Stokes-Einstein equation. A simple correlation for a wide range of proteins is [6]:

$$r = 0.88 \cdot MW^{1/3} \tag{3}$$

where r is the radius in nm and MW is the protein molecular weight in kDa (kilo Daltons). The hard sphere radius of human insulin with a molecular weight of 5.8 kDa is 1.6 nm while that for a 155 kDa monoclonal antibody is 4.7 nm.

The effective radius of a protein in the context of membrane separations can be considerably larger than the hard sphere radius due to the presence of the diffuse ion cloud (the electrical double layer) that surrounds the charged protein in aqueous solution [14]. This effect can be quite dramatic, with the effective molecular weight of the protein (as determined by size exclusion chromatography) increasing by more than a factor of 20 as the solution ionic strength is reduced from 150 to 5 mM [15].

2.2. Feedstock characteristics

Biotechnology products (typically proteins or DNA) are produced with recombinant DNA in cultures of cells, transgenic animals, or transgenic plants. Common cells used for production include Chinese Hamster Ovary (CHO) cells, *E. coli* bacteria, and yeast. Cell-based production systems are typically carried out in batch mode although a small number of perfusion systems are also in use. Final manufacturing scale fermentation is carried out at 1000–100,000 L scale with the majority of CHO based fermenters in the 8000–25,000 L scale. Transgenic animals have been explored as alternative production systems, including goats and pigs, with the recombinant products harvested in the animal's milk [16]. Transgenic eggs have also been developed. Several transgenic plant systems have been examined including corn and tobacco [17]. Cell-free systems are also being developed [18].

Product titers have increased dramatically over the past 30 years. Current cell culture systems typically yield product concentrations between 1 and 3 g/L while concentrations of 10 g/L have been obtained in transgenic milk. The detailed composition of the initial feedstock depends strongly on the source material. For cell culture systems, the critical impurities are the host cells, host cell proteins, DNA, lipids, and other cell debris. This may include a variety of proteolytic enzymes that can degrade the desired product. The cell culture media can also be highly complex, including a variety of growth factors, nutrients, stabilizing agents, and antifoams. The downstream process must also be designed to remove endogenous virus-like particles that may be present in genetically-engineered mammalian cell lines as well as adventitious viruses introduced during processing. Transgenic milk contains high concentrations of fat and normal milk proteins. Of particular concern are the caseins, which form large micelle structures that can trap product.

2.3. Overview of processing applications

Membranes are used extensively throughout the production, purification, and formulation of biotechnology products. Upstream applications include sterile filtration (Section 3) of fermentation media, pH control solutions, and gases (air, oxygen, and off-gases). Filters with 0.1 μm pore size provide retention of both mycoplasma as well as larger organisms. Depth filtration (Section 5) may also be used for turbid feed streams such

as peptone solutions. Tangential flow microfiltration (Section 4) is used for medium exchange (4.e.i), perfusion (4.e.ii), and harvest (4.e.iii). Virus filtration (Section 6) may be used to protect cell cultures from introduction of viral contaminants in media raw materials. Ultrafiltration (Section 8) and diafiltration have been used to remove glycine, hypoxanthine, and thymidine from serum to provide selective pressure on serum dependent cell cultures.

Downstream applications include sterile filtration (Section 3) of buffers, products, and gases (typically air and nitrogen). Depth filtration (Section 5) may also be employed for product feed streams that are particularly difficult to filter with other types of membranes. Virus filters (Section 6) are often used in the downstream processing of cell culture derived products to insure removal of both endogenous virus particles as well as any adventitious viruses that may enter into the cell culture through contaminated raw materials. Virus filtration was initially implemented as a tangential flow filtration operation (Section 6.3.1) but is now typically performed by normal flow filtration (Section 6.3.2). Membrane chromatography (Section 7) can be used for purification of both products and raw materials. For example, it may be advantageous to remove endotoxins from raw materials before using them in the downstream process. Ultrafiltration is used to concentrate and buffer exchange product pools throughout the downstream process. It is also used as the method of choice for final formulation of bulk product.

2.4. Requirements for the biotechnology industry

Purity requirements for human pharmaceutical protein products are focused on host cell proteins, product variants, DNA, viruses, endotoxins, resin and membrane leachables, and various small molecules used in the fermentation and purification processes [19]. Acceptable host cell protein levels are determined by the manufacturer based on process capability and safety testing in toxicology and clinical trials combined with review by regulatory agencies. Typical targets for monoclonal antibody products are in the ppm range (micrograms of host cell proteins per gram of antibody product). Product aggregate levels are controlled to minimize the potential for an enhanced immunogenic response in patients arising from the presentation of repetitive structural elements within the aggregate [20]. While the acceptable level will depend on the specific product, it is common to maintain aggregate levels below 5%. Protein product variants may include deamidated and oxidized forms as well as various glycosylation forms [21]. Acceptable levels of these forms will depend on bioactivity, safety, and efficacy testing in clinical trials. DNA levels are set by the World Health Organization at $\leq 10\,\mu g$ per dose.

Regulatory guidelines require that recombinant DNA derived protein products for human use meet a criterion of less than 1 virus particle per million doses. There is also a requirement to demonstrate that virus inactivation and clearance are accomplished using at least three different mechanisms. Common methods for removal of viruses include sized based filtration and affinity and anion exchange chromatography. Methods for inactivation often include low pH, heat, and use of solvents and detergents. Endotoxin limit levels are usually set to less than 5 EU/kg of patient weight. Membrane and resin leachable levels are determined by the end-user with limits typically set at ≤ 1–$10\,\mu g/mL$. Acceptable final levels of small molecules used in the process (but absent from the product formulation) are determined based on toxicity and regulatory guidelines. Microbial contamination is controlled throughout both upstream and downstream processes. Sterility is required for fermentation and final product. Sterility is often not possible during the purification process due to the lack of steamable resins and membranes and technical challenges with regard to thermal expansion and contraction of various materials of construction. Microbial levels are, however, controlled using steam sterilized $0.2\,\mu m$ filters and steam sterilized product pool tanks at each stage of the process.

3. Sterile filtration

3.1. Principles

Almost all biotherapeutics are processed by sterile filtration since the thermal stability of these molecules prohibits the use of alternative sterilization methods. Sterile filters operate using normal flow filtration, with bacteria, cell debris, and insoluble aggregates retained by the membrane. These filters are used to remove bacteria and particles from feedstock solutions, to protect downstream units from fouling by insoluble materials, and for sterile fill operations.

The capacity of the filter is determined by the fouling characteristics of the feed solution. Fouling can occur on the upper surface of the membrane, both by pore blockage and by the formation of a cake or deposit, and also within the membrane pore structure. Fouling causes a decay in flow rate for constant pressure operation and it increases the pressure for operation at constant filtrate flux.

3.1.1. Classical fouling models

Flux decline data are typically analyzed using one of the classical filtration models: standard pore blockage, intermediate pore blockage, pore constriction, and cake filtration [22]. The governing equations for the filtrate flow rate (Q) during constant pressure operation and the transmembrane pressure (P) during constant flow operation are summarized in Table 1. The results are expressed in terms of the filtration time (t) and the cumulative filtrate volume (V). The linearized forms are convenient for data analysis and model identification. In each case, the rate of fouling is assumed to be proportional to the rate at which the foulant material is brought to the membrane by the filtrate flow, neglecting any back-transport or detachment mechanisms. In the cake filtration model, fouling results in a deposit on the external surface of the membrane that provides an additional resistance to flow in series with that of the membrane. In the other three models, the membrane is assumed to be composed of a parallel array of cylindrical pores with uniform pore size. In the pore constriction model, fouling occurs within the membrane leading to a reduction in the effective pore size. The standard and intermediate pore blockage models assume that the pores are occluded by the foulant, with the intermediate blockage model

Table 1
Governing equations for flux decline models

Constant pressure	Flow rate	Linearized form
Pore blockage	$\dfrac{Q}{Q_0} = \exp(-\beta t)$	$\ln(Q) = at + b$
Intermediate blockage	$\dfrac{Q}{Q_0} = (1 + \beta t)^{-1}$	$\dfrac{1}{Q} = at + b$
Pore constriction	$\dfrac{Q}{Q_0} = (1 + \beta t)^{-2}$	$\dfrac{t}{V} = at + b$
Cake filtration	$\dfrac{Q}{Q_0} = (1 + \beta t)^{-1/2}$	$\dfrac{t}{V} = aV + b$

Constant flux	Pressure	Linearized form
Pore blockage	$\dfrac{P}{P_0} = (1 - \beta t)^{-1/2}$	$\dfrac{1}{P^2} = a - bV$
Intermediate blockage	$\dfrac{P}{P_0} = (1 - \beta t)^{-1}$	$\dfrac{1}{P} = a - bV$
Pore constriction	$\dfrac{P}{P_0} = (1 - \beta t)^{-2}$	$\dfrac{1}{P^{1/2}} = a - bV$
Cake filtration	$\dfrac{P}{P_0} = 1 + \beta t$	$P = a + bV$

Fig. 2. V_{max} analysis for BSA filtration through 0.2 μm polycarbonate track-etch (PCTE) and 0.2 μm polyvinylidene fluoride (PVDF) membranes. Solid curves are model calculations from [25]. Dashed curves are linear regression fits using data obtained for $t < 10$ min.

allowing for particle superposition on the external membrane surface.

3.1.2. Pore blockage—cake filtration model

Although many investigators have used the simple fouling models to analyze flux decline data, there is considerable experimental evidence that there is often a transition in fouling behavior during a filtration run, with the initial flux decline associated with pore constriction and/or pore blockage (possibly in sequence) followed by cake formation. Ho and Zydney [23] developed a combined pore blockage—cake filtration model that accounts for this transition. Protein aggregates and cell debris are assumed to deposit on the membrane surface blocking the pores, but this initial deposit is assumed to be at least partially permeable to fluid flow. A cake layer or deposit then begins to form over those regions of the membrane that have already been "blocked" by the initial deposit. Ho and Zydney [23] showed that the filtrate flow rate can be approximated as:

$$\frac{Q}{Q_0} = \exp(-\beta t) + \frac{R_m}{R_m + R_p}[1 - \exp(-\beta t)] \tag{4}$$

where R_m is the resistance of the clean membrane (equal to $1/L_p$) and R_p is the resistance of the growing deposit:

$$R_p = (R_m + R_{p0})\sqrt{1 + \alpha t} - R_m \tag{5}$$

R_{p0} is the resistance of the initial deposit and α is proportional to the specific resistance of the growing cake. Eqs. (4) and (5) have been shown to provide a much better description of fouling by protein aggregates than the classical filtration models [23].

The general framework underlying the combined pore blockage—cake filtration model has been extended to begin to account for the effects of the complex pore morphology in current sterile filtration membranes, including both the asymmetric structure [24] and the pore interconnectivity [25]. The interconnected pore structure allows fluid to flow under and around any pore blockage, significantly reducing the rate of flux decline relative to that for a membrane with straight-through non-interconnected pores.
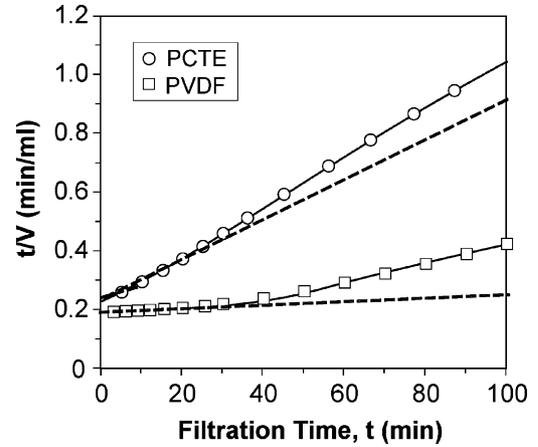
3.1.3. V_{max} and P_{max} analysis

The simplest approach to sizing normal flow filters is the flow decay method, in which the cumulative filtrate volume is measured through a small-area test filter until the flow rate drops to 10% (or 20%) of its initial value. These data are then extrapolated to larger production volumes assuming that the filter performance scales linearly with membrane area. The disadvantage to this approach is that large volumes of process fluid are required to achieve the 80% or 90% reduction in flux, severely limiting the amount of testing that can be conducted in a time and cost effective manner, particularly during early stages of product development where feedstock availability is highly limited.

An alternative to the flow decay method is the V_{max} analysis [26]. In this case, flux decay data are obtained over only a short filtration time (typically 10–15 min), with the data extrapolated to longer filtration times using the linearized form of the pore constriction model (Table 1):

$$\frac{t}{V} = \frac{1}{Q_0} + \left(\frac{1}{V_{max}}\right)t \tag{6}$$

The inverse of the slope on a plot of t/V versus t is the maximum volume of fluid that can be filtered before the membrane is completely plugged. Scale-up is then accomplished by assuming that the available capacity (usually between 50 and 80% of V_{max}) scales linearly with the membrane area. The V_{max} method requires smaller volumes of process fluid and shorter testing times, but it may lead to large errors in predicted capacity if fouling is not due to pore constriction [25].

Fig. 2 shows a typical V_{max} plot for filtration of BSA through a track-etch polycarbonate and polyvinylidene fluoride (PVDF) membranes. The PVDF membrane has a much higher capacity (lower slope) due to its high degree of pore interconnectivity. The linear fit to the data for the PVDF membrane significantly underestimates the capacity; thus, considerable care must be taken in properly interpreting and using this type of V_{max} analysis.

A similar approach can be used for scale-up for operation at constant filtrate flux. In this case, the total resistance, equal to the ratio of the transmembrane pressure to the flux, is plotted as a function of the volume filtered per unit membrane area. If fouling is due entirely to pore constriction, the pressure (*P*) will increase with cumulative filtrate volume (*V*) as (Table 1):

$$\frac{P}{P_0} = \left(1 - \frac{V}{V_{max}}\right)^{-2} \tag{7}$$

where P_0 is the initial pressure and V_{max} is the filtrate volume corresponding to complete saturation of all pores. A similar equation can be derived based on the pore blockage model, but with an exponent of -1 instead of -2. The capacity is typically defined based on a pre-determined pressure end-point. Alternatively, the end-point may be defined based on measurements of the filtrate turbidity if there is significant breakthrough of debris at high loadings. The P_{max} method provides much more reliable scaling than V_{max}, and the use of constant filtrate flux is highly attractive for direct flow operations.

3.2. Membranes

Sterile filters typically encompass 0.1 and 0.2 μm pore size filters, both of which meet specific standards for removal of microorganisms. Sterile filtration criteria for 0.2 μm filters are based on removal of 10^7 colony forming units (CFU) of Brevimunda Diminuta per cm² of membrane area [27]. These membranes are typically used throughout the purification process for recombinant DNA derived proteins. Cell culture operations may use 0.1 μm membranes to provide protection against mycoplasma [28] that may be present in various raw materials.

Sterile filtration membranes have been made from a variety of base polymers including polyethersulfone (PES), polyvinylidene fluoride, nylon, and polypropylene (PP). Many of these base membranes also have surface coatings or are cast as polymeric alloys to reduce product protein adsorption and to reduce fouling in general. These chemical modifications often focus on rendering the membranes more hydrophilic and lowering the zeta potential to avoid ionic interactions. Significant yield losses due to protein adsorption are, however, rare even with highly hydrophobic chemistries such as unmodified PP [29].

Sterile filters have the ability to remove microorganisms by size exclusion and to remove protein aggregates by both size exclusion and adsorption. The latter characteristic is often as important as the removal of microorganisms. Protein aggregates typically form over time even during product hold steps between downstream unit operations. In addition, higher levels of aggregation will occur in steps such as ultrafiltration when the protein is subjected to multiple passes through pumps and valves. Fortunately, microcavitation primarily leads to the generation of insoluble aggregates that are easily removed during sterile filtration. While significant turbidity may be observed after some downstream processing operations, this is due to the strong dependence of light scattering on the particle radius. Static light scattering intensity, in which the intensity is measured as a function of scattering angle, is proportional to r^3 while the dynamic light scattering signal, obtained from the temporal variation of the intensity, is proportional to r^6 where r is the particle radius. Yield losses due to the generation of insoluble aggregates are usually less than the limit of quantification. The generation of soluble product multimers during downstream processing is also rare. Contrary to common belief, the aggregation that does occur is not due to shear per se but is instead due to microcavitation that occurs in pumps and valves. Microcavitation leads to protein–air interfaces that in turn lead to protein denaturation and aggregation. There is also evidence that such denaturation can often be eliminated if the air is replaced with nitrogen (oxygen and other gases can be removed by nitrogen sparging followed by a nitrogen overlay). While protein aggregate adsorption and retention become capacity limiting for feed streams with low microbial levels, the removal of such aggregates should be considered as an important part of the purification process. This is especially true for filtration of final bulk product. Further aggregation after the last step in the process is avoided by proper development and implementation of formulation buffers and excipients.

In addition to the use of many different polymers, manufacturers have the ability to cast a number of different membrane structures. Various production methods are used depending on both the polymer and the desired structure. Methods include air casting, immersion casting, melt casting, track-etching, stretching, and radiation-induced polymerization [6]. Casting may also be performed using another membrane as a substrate, often referred to as composite membranes. The structural characteristics of the membrane play a major role in determining permeability, retention capability, process flux, and process capacity. Recent developments in the production of composite and multi-layer membranes have provided dramatic increases in membrane capacity compared to the isotropic membranes used for sterile filtration in early bioprocesses.

3.2.1. Isotropic membranes

Isotropic membranes have a uniform structure throughout the depth of the membrane as shown in Fig. 3A. Permeability is primarily determined by the pore size distribution and the thickness of the membrane. When filtering particles larger than the pore size, process capacities may be limited since retention is at the surface of the membrane. High levels of clearance may, however, be achieved with particles that either adsorb to or are trapped by the entire membrane structure.

3.2.2. Anisotropic membranes

Anisotropic membranes have a graded pore size distribution that varies throughout the depth of the membrane as shown in Fig. 3B. Permeability can be enhanced with these structures while still maintaining the mechanical strength of the membrane. Process capacities may also be enhanced for feed streams that have a wide particle size distribution since different particle sizes may be retained by different layers within the membrane. Anisotropic membranes may also be used with the smaller pore size on the upstream side. This can be advantageous for feed streams with relatively homogeneous particle size distribution and small loads where surface retention is adequate and the rest
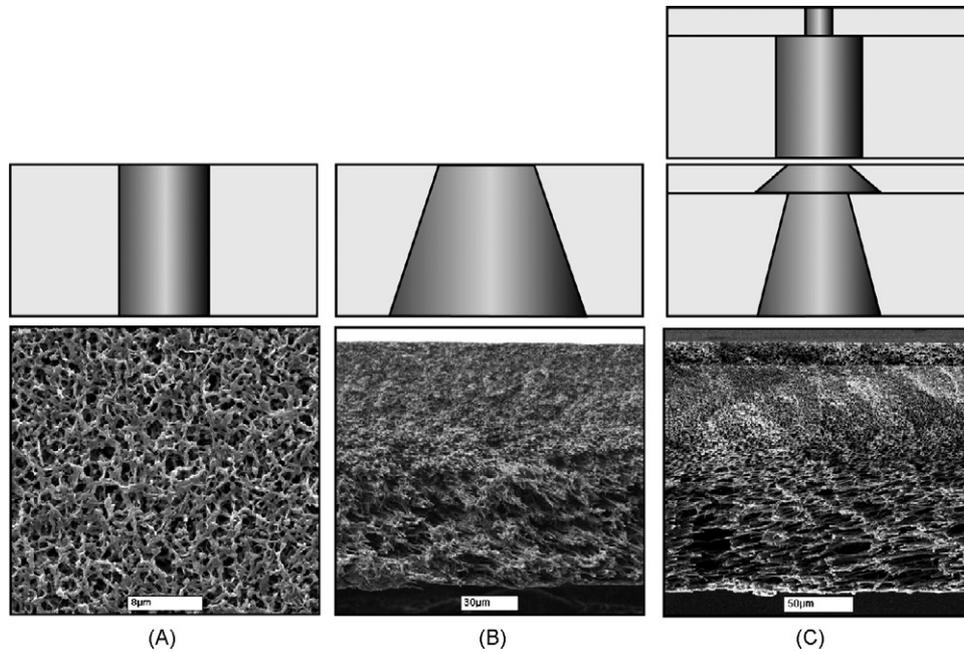
Fig. 3. Evolution of casting technology for sterile filters showing progression from (A) isotropic to (B) anisotropic to (C) co-cast structures. High capacity sterile filters have been developed for the biotechnology industry using multiple composite membranes with varying pore size distribution. Scanning electron micrographs used with permission of Millipore Corporation.

of the membrane only serves as a mechanical substructure with increased permeability compared to an isotropic membrane with the same retention capability.

3.2.3. Composite membranes

Composite membranes combine two different structures into a single membrane as shown in Fig. 3C. The different layers can be independently formed with either an isotropic or anisotropic morphology, with each having a distinct pore size distribution, aspect ratio (ratio of pore sizes on the two faces of the membrane), and thickness. This provides many degrees of freedom to tailor the structure to various types of feed streams. One of the membrane layers may also be designed as a built-in pre-filter for the second layer.

3.2.4. Multi-layer membranes

In addition to using composite membranes it can be beneficial to physically layer two different membranes together, each of which is cast separately with the desired pore size and surface characteristics. The first layer is typically used as a pre-filter while the second layer is an absolute rated filter with either a 0.1 or 0.2 μm rating depending on the application.

3.3. Modules

3.3.1. Code 7 cartridges

The most common sterile filtration cartridge used in the biotechnology industry today is a "Code 7" design, which primarily refers to the bottom adapter that has two o-rings and two tabs that lock into corresponding grooves in the bottom of the stainless steel housing. Code 7 cartridges are provided in 10, 20, 30, and in some cases 40 in. high configurations. The larger

sizes are obtained from 10 in. elements that are fused together before adding the top and bottom adapters.

3.3.2. Other cartridge types

In addition to Code 7 style cartridges various other filter elements are available from membrane manufacturers for applications requiring less membrane area. These designs are specific for each manufacturer and require the use of the corresponding housing design.

3.3.3. Pleating technology

Improved scale-up and process economics can be obtained both by using novel membrane structures and by increasing the packing density of membrane inside the cartridge. An example of improved packing density is shown in Fig. 4 for a pleated membrane. Packing densities that are approximately twice as high as traditional cartridges are obtained by using longer pleats that are rotated into a tight pack. Intermediate polymer screens are used to avoid blinding of the membrane surface. The increased membrane area has several benefits including higher capacity (per 10 in. element), lower flux (which also increases capacity), and smaller housings. Smaller housings save capital, labor, and manufacturing turn-around time since larger housings require longer steaming and cooling times and are more difficult to handle.

3.4. Equipment

3.4.1. Stainless steel housings

Stainless steel housings are provided in various sizes including single cartridge, 3-round, 5-round, 6-round, 9-round, 12-round, and larger sizes. Code 7 cartridge and housing designs

Star Pleat™   Ultipleat™
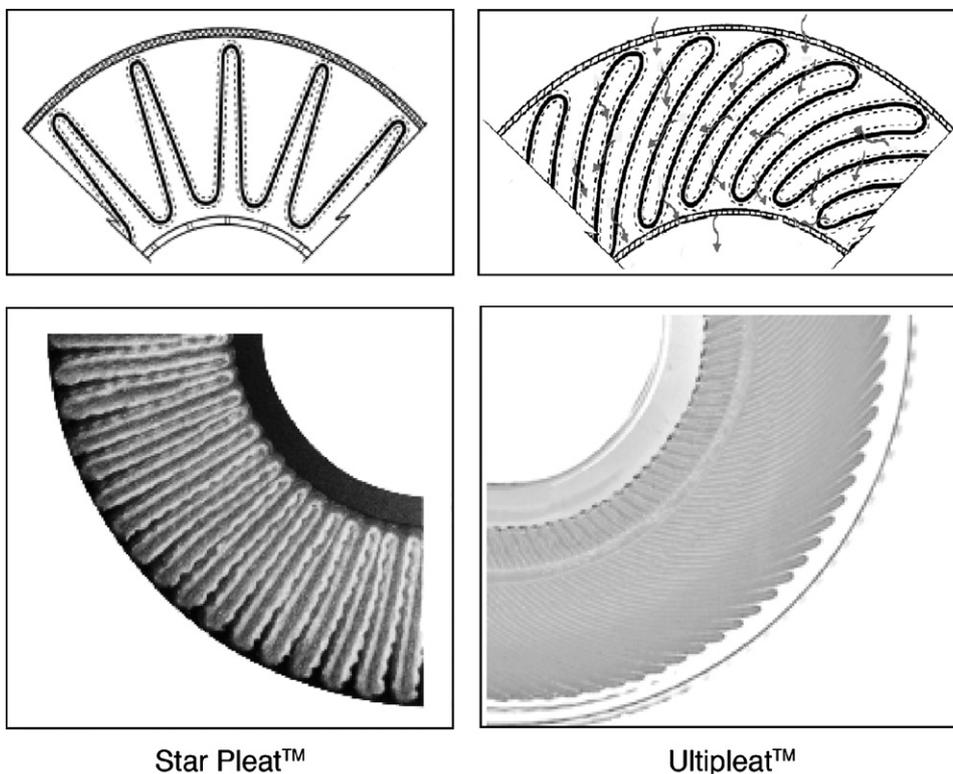
Fig. 4. Comparison of packing density for Pall Fluorodyne EX high capacity sterile filter using Ultipleat® technology (1.1 m² per 10 in. cartridge) with that of a conventional filter using Star Pleat™ (0.7 m² per 10 in. cartridge). Photos used with permission of Pall Corporation.

from different manufacturers do not share a common set of specifications and tolerances. It is therefore imperative that compatibility of cartridge and housing designs are verified for any installation. Verification may include checks on minimum and maximum dimensions for the cartridge and housing, installation tests, integrity tests, and actual microbial challenges with housings built to maximum dimensions and cartridges specifically machined or molded to minimum dimensions.

3.4.2. Capsules

Sterile filters are also provided in various self-contained cartridges that do not require the use of stainless steel housings. For example, Pall makes KleenPak™ capsules using thermally bonded components to minimize leachables from adhesive sealants. These capsules are pre-sterilized by gamma irradiation.

3.5. Processes

Sterile filter applications can be divided into flux limited and capacity limited cases. Flux limited applications usually include purified water and simple solutions such as buffers and media, although some of these may contain sufficient particulate material to become capacity limited. Most other feed streams are capacity limited, with the maximum capacity dependent on the operating conditions. Studies need to be performed to establish an optimum flux that results in a filter size that can both process a given volume in a given amount of time while providing adequate capacity. A safety factor of 1.5 is typically added to the measured capacity to account for process variability. Larger

safety factors may be warranted for more variable feed streams such as harvested cell culture fluid.

Capacity studies are performed using either constant pressure or constant flux. The appropriate study will depend on the intended mode of filtration. Constant flux will typically result in higher throughput capacities. Examples of constant flux capacity studies are shown in Fig. 5. The composite PES membrane has
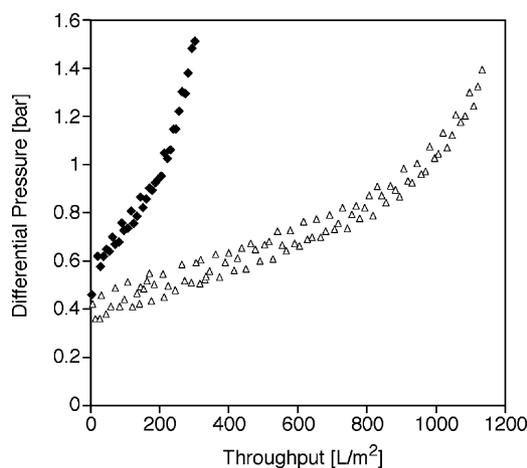
Fig. 5. Capacity studies showing pressure vs. throughput at constant filtrate flux for composite anisotropic 0.2 μm PES membrane with co-cast anisotropic 0.5 μm pre-filter (Millipore Express® SHC membrane) run at a flux of 1295 L/m²/h (open symbols) and isotropic 0.2 μm hydrophilic PVDF membrane (Millipore Durapore® membrane) run at a flux of 927 L/m²/h (closed symbols). Data obtained with a monoclonal antibody Protein-A affinity chromatography pool with the fluxes corresponding to the same flow rate per 10″ Code 7 element. Data obtained by Jean Luo and Robert van Reis at Genentech, Inc.

more than four times the capacity of the isotropic PVDF membrane when used to clarify a monoclonal antibody feedstock (obtained after a Protein A affinity chromatography step).

Determining the optimum membrane structure and the optimum combination of pre-filter and final filter for any given application relies heavily on empirical testing. Comparing experimental data to filtration models can, however, provide insights into fouling mechanisms that in turn may guide the development or selection of better membranes or filter combinations. Efforts are also underway to develop empirical correlations between the pore size distribution, particle size distribution, and process capacity performance.

Scale-up should include side-by-side capacity studies comparing performance data obtained on discs, capsules and pleated cartridges due to the very different internal flow patterns and pressure distributions in these modules. Disc studies with 47 mm diameter discs are done to conserve material while verification studies on 1-in. cartridges are done to ensure scalability.

4. Tangential flow micro-filtration

4.1. Principles

Tangential flow microfiltration competes with centrifugation, depth filtration, and expanded bed chromatography for the initial harvest of therapeutic proteins from mammalian, yeast, and bacterial cell cultures [29]. Tangential flow microfiltration using 0.2 μm pore size membranes generates a filtrate solution that requires no further clarification; competing technologies are used in conjunction with normal flow (usually depth and sterile) filters to achieve the high levels of cell and debris removal needed to protect subsequent chromatography columns. Recent trends towards higher density cell cultures, which tend to have much higher levels of cell debris, have created major challenges in the application of microfiltration for initial clarification.

The behavior of tangential flow microfiltration systems is typically dominated by concentration polarization and fouling effects, with the filtrate flux limited by the accumulation of a concentrated layer of cells and cell debris at the membrane surface [30]. These phenomena can be avoided by operating at low filtrate flux (below the critical flux for fouling) and/or by exploiting inertial lift effects to maintain a particle-free zone near the membrane. At steady-state, the rate of cell transport to the membrane is balanced by the rate of back-transport. Brownian diffusion is negligible for large cells and debris, thus the rate of back-transport is determined by the effects of shear-induced diffusion and/or inertial lift.

4.1.1. Shear-induced diffusion

Shear-induced diffusion refers to the random, diffusive motion, arising from particle–particle interactions in the shear flow of a concentrated suspension. The shear flow causes particles on neighboring streamlines to interact or "collide", leading to transient displacements perpendicular to the flow. Zydney and Colton [31] used a simple stagnant film model to evaluate the pressure-independent filtrate flux accounting for the effects of
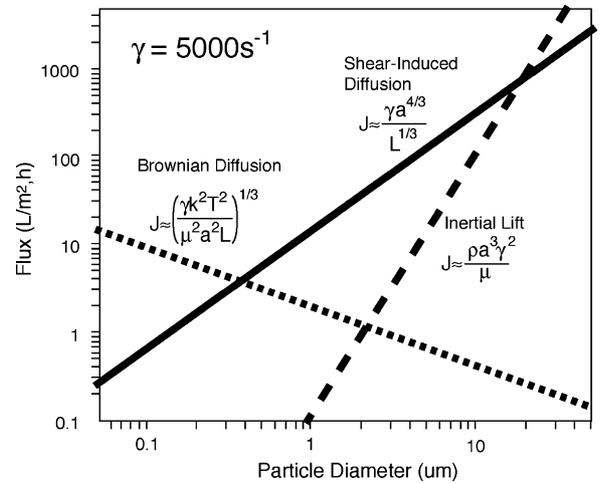
Fig. 6. Comparison of predicted filtrate flux based on the Brownian diffusion, shear-induced diffusion, and inertial lift models. Calculations were performed for a nominal wall shear rate of $5000\,\mathrm{s}^{-1}$ and $L = 0.2\,\mathrm{m}$ [30].

shear-induced diffusion:

$$J = 0.070 \left(\frac{a^4}{L}\right)^{1/3} \gamma_w \ln\left(\frac{C_w}{C_b}\right) \qquad (8)$$

where a is the particle (cell) radius, L the channel length, γ_w the local shear rate at the membrane surface, and C_w and C_b are the particle concentrations at the membrane (wall) and in the bulk suspension, respectively. Good agreement with experimental data were obtained using $C_w = 0.95$ by volume fraction for deformable red blood cells. The C_w value for more rigid cells will be closer to 0.7. Eq. (8) can be used in multi-component systems to describe the polarization of each component, with C_w and C_b the concentrations for each species. For a typical module ($L = 30$ cm, $\gamma_w = 4000\,\mathrm{s}^{-1}$), the stable operating flux for a system with a high level of cell debris ($a = 0.5\,\mu\mathrm{m}$, $C_w/C_b \approx 1000$) is about 9 LMH (L/m²/h).

4.1.2. Inertial lift

Inertial lift arises from hydrodynamic interactions associated with the distortion of the fluid streamlines in the gap between the particle and the flow boundary [30]. The inertial lift velocity is proportional to the cube of the particle radius and the square of the local shear rate. It typically dominates shear-induced diffusion as a mechanism for back transport for particles greater than 10 μm in radius [30].

Fig. 6 shows a comparison of the predicted flux using the polarization analysis based on Brownian diffusion, shear-induced diffusion, and inertial lift as a function of the particle radius. Brownian diffusion dominates for proteins while shear-induced diffusion is most important for cells and cell debris ($0.4\,\mu\mathrm{m} < a < 15\,\mu\mathrm{m}$). Inertial lift is only significant for flocculated or aggregated cells.

4.1.3. Critical flux analysis

Field et al. [32] originally introduced the concept of a "critical flux" based on an analysis of data for the tangential flow microfiltration of yeast cell suspensions. The critical flux hypothesis is

that there exists a flux below which fouling is negligible and there will be no measurable decline in flux (or increase in transmembrane pressure) with time. The value of the critical flux depends on the device hydrodynamics as well as any long-range (e.g., electrostatic) interactions between the particles and membrane. Several recent studies have shown that a low level of fouling can take place even below the critical flux [33]. Fouling under these conditions may be due to the heterogeneous distribution in the local flux over the surface of the membrane, with high local flow rates through certain regions resulting in local fluxes that exceed the critical flux [34].

4.2. Membranes

4.2.1. Hollow fiber

Narrow bore hollow fiber membranes for tangential flow microfiltration are made from a variety of polymers including polyethersulfone, polysulfone, polypropylene, polyvinylidien fluoride, and mixed cellulose esters. These fibers typically have inner diameters of 0.2–1.8 mm, providing laminar flow with moderate shear rates. Most hollow fibers have an asymmetric structure with the dense skin at the lumen side of the fiber. The fibers are self-supporting, so they can typically be cleaned by back-flushing from the filtrate-side. Pre-sterilized disposable hollow fiber modules have also been developed, eliminating the need for cleaning and regeneration.

4.2.2. Flat sheet

Flat sheet membranes are typically cast on a non-woven substrate and can have either an isotropic or asymmetric structure [6]. A variety of polymers are available, including polysulfone, polyethersulfone, cellulose, and hydrophilized polyvinylidene fluoride. These materials are often surface modified to increase hydrophilicity and reduce fouling, and they can be cast as mixed polymers (e.g., with polyvinylpyrrolidone to increase wetability). Membranes can be directly bonded or glued to plates or sealed using appropriate gaskets. Open channel systems are commonly employed for tangential flow microfiltration to minimize plugging by cell aggregates and debris.

4.3. Modules

4.3.1. Non steam-in-place (SIP)

Tangential flow microfiltration modules are used for both sterile and non-sterile processes. Several sterilization methods are possible including chemical, super heated water, autoclave, and steam-in-place. An example is the Akzo autoclavable MF cartridge as shown in Fig. 7. This product provides a good hollow fiber membrane for cell-protein separation. The combination of fiber inner diameter (0.6 mm), fiber length (435 mm), and pore size (0.2 μm) provides good fluid dynamic properties with regard to feed flow rate (183 L/m²/h as normalized by the membrane area), wall shear rate (4000 s^{-1}), and pressure drop (25 kPa) while providing a sterile barrier. The original product could not be sterilized by thermal means. Five modifications were made to enable autoclave sterilization. The materials of construction were maintained with a polypropylene fiber

Fig. 7. Autoclavable hollow fiber cartridge with: (1) annealed polypropylene to eliminate polymer stress; (2) smaller diameter to reduce thermal expansion and contraction; (3) serrated bonding surface between polyurethane potting compound and polypropylene cartridge; (4) increased thickness of cartridge cage; and (5) inserted metal ring in cartridge outlet (not shown) to stabilize seal during heating and cooling. Photo used with permission of Genentech, Inc.

potted in polyurethane within a polypropylene cartridge. The unmodified polypropylene hollow fiber membrane worked very well for mammalian cell–protein separation despite the hydrophobic chemistry. To enable autoclave sterilization the polypropylene components were annealed to reduce stresses in the polymer. The outer cage of the cartridge was also strengthened by a thicker design to withstand heating and cooling cycles. The cartridge diameter was made smaller to reduce the absolute differences in thermal expansion and contraction of the polypropylene and polyurethane components. The bond between the polypropylene and polyurethane was improved by replacing a flat interface with a jagged design. Finally, a stainless steel ring was inserted into the entrance and exit connectors to stabilize the dimensions and ensure adequate o-ring sealing
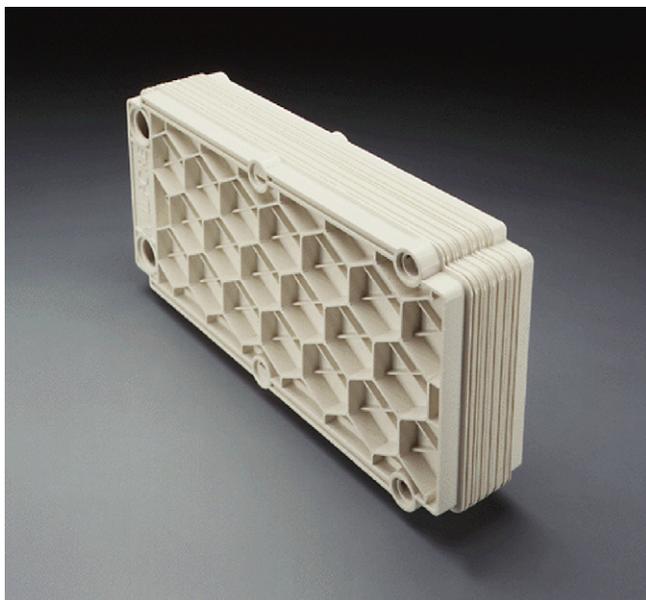
Fig. 8. Prostak[TM] MF stacked plate tangential flow microfiltration module developed for steam-in-place applications. Membranes are integrally bonded to both sides of a rectangular plate, which serves as the permeate carrier. Multiple plates are then bonded together to form an open channel plate and frame type device. Introduced by Millipore in 1985. Photo used with permission of Millipore Corporation.

against the stainless steel housing. Stainless steel systems with up to 264 ft^2 of membrane area can be successfully autoclaved. After autoclaving, the systems were connected to fermenters by stainless steel pipe and all connections were steamed-in-place to provide a sterile cell-protein separation system (see Section 4.5.1 Medium Exchange). In principle, these cartridges could also be sterilized by other thermal means including super-heated water and steam-in-place. Autoclaves and steam-in-place systems are more commonplace in the biotechnology industry. SIP of a hydrophobic membrane carries with it the risk of having to re-wet the fibers under sterile conditions.

4.3.2. Steam-in-place

The most convenient method for sterilization of large-scale industrial MF systems is steam-in-place. SIP MF modules were specifically developed for sterile cell-protein separations. An example of such a module is the Millipore Prostak[TM] cartridge as shown in Fig. 8. Cartridges are available with 0.2, 0.45, and 0.65 μm PVDF membranes with a hydrophilic hydroxypropylacrylate surface chemistry. The final SIP product uses a glass-filled polysulfone cartridge material to withstand thermal expansion and contraction while maintaining an integral bond with the membrane and sterile seals to the stainless steel end-plates.

4.4. Processes

4.4.1. Medium exchange and perfusion

TFF MF systems can be used to carry out cell-protein separation processes including medium exchange during fermentation. The process was originally developed for the production of recombinant human tissue-type plasminogen activator (TPA) at Genentech. Chinese hamster ovary (CHO) cells were grown in successively larger seed fermenters with media containing serum to support cell growth. Performing the final production fermentation in the presence of serum proteins, however, resulted in several unique difficulties. High molecular weight complexes were formed between TPA and serum proteins. Several proteolytically cleaved forms of TPA were also generated in the presence of serum. Improved yield and product quality were achieved by developing a process in which the cells could be grown in serum-containing media throughout the cell culture seed train but then switched to a serum-free media for production. The penultimate cell culture (2400 L) was first concentrated six-fold and then media exchanged with 6 diavolumes of serum-free media using a sterile TFF MF system with either 24.5 m^2 of 0.2 μm autoclaved Akzo polypropylene hollow fibers or 18.6 m^2 of 0.65 μm SIP Millipore Durapore® polvinylidene fluoride flat sheet membranes. The media exchanged cells were subsequently transferred to a 12,000 L production fermenter operated with serum-free media. Both TFF systems used a wall shear rate of 4000 s^{-1} and a flux of 50 L/m^2/h. Cell viability was maintained at very high levels. Sterile TFF MF systems developed for medium exchange can also be used for perfusion culture. Perfusion is a culture production method in which product is continuously removed and replaced with new media.

4.4.2. Harvest

The same MF technology that was originally developed for medium exchange has also been used to harvest recombinant DNA derived proteins from both mammalian and bacterial cultures. Harvest systems are generally larger due to the larger scale of production fermenters. A 174 m^2 hollow fiber system is shown in Fig. 9A and a 186 m^2 flat sheet system is shown in Fig. 9B. These systems have been used for harvest of proteins from CHO cultures with the same wall shear rate as medium exchange processes (4000 s^{-1}) but at lower flux rates (around 26 L/m^2/h) due to the higher cell debris load [29]. The smaller pore size membrane enabled direct sterile filtration into the harvested cell culture fluid (HCCF) hold tank whereas the larger pore size membranes required the use of depth filters prior to sterile filtration of the HCCF. The larger membrane pore size was required to achieve sufficient process capacity (114 L/m^2 including a 1.5x safety factor) on more challenging feed streams. Yields averaged 99% and membranes could be re-used 100 times [29].

5. Depth filtration

5.1. Principles

Cells and debris are removed in depth filtration throughout the filter media, in contrast to the surface removal (screening) typically observed with microfiltration membranes. Depth filtration has been successfully employed for the clarification of monoclonal antibody solutions [35,36]; for removal of particulates and contaminants from acidified protein solutions prior to chromatographic processing [37]; and for removal of DNA from

(A)

(B)

Fig. 9. Large-scale microfiltration systems for harvest of recombinant DNA derived proteins from Chinese Hamster Ovary Cells. (A) Microdyn 0.2 μm polypropylene hollow fiber microfiltration system with 174 m² membrane area. (B) Millipore Prostak™ flat sheet membrane system with 186 m² of 0.65 μm pore size hydrophilic PVDF membrane. Photos used with permission of Genentech, Inc.

Fig. 10. Millipore depth filter cartridge with two depth filters of different grades and a final layer of cellulose acetate pre-filter. Photo used with permission of Millipore Corporation.

mammalian cell cultures [38]. Depth filters are typically used in conjunction with normal flow sterile filters, providing a cost-effective process due to the large increase in capacity of the sterile filter. This is particularly true for heavily fouling feed stocks.

Particle removal in depth filtration occurs by a variety of mechanisms. Cells and cell debris can be removed by physical capture in narrow pore spaces. Multi-layer structures with graded pore size provide the capability of removing different size debris within different layers of the filter. Electrostatic interactions are critically important for the capture of charged species. Positively-charged depth filters can provide very high removal of negatively-charged DNA, viruses, and endotoxin [38]. Other effects such as hydrophobic interactions can also be important.

5.2. Filter media

Depth filters employed in bioprocessing are usually composed of cellulose or polypropylene fibers with an appropriate filter aid (e.g., diatomaceous earth, perlite, or activated carbon) and a binder. Charged filters can be formed by incorporating charged polymers or ion exchange particles within the filter [39].

Multi-layered depth filters have been developed to improve the particle removal capabilities, with each layer having a unique pore size, electrical charge, and surface chemistry (Fig. 10). Integral filters with a membrane as the bottom layer provide even higher levels of particle removal.

5.3. Equipment

Depth filters are typically made available in 47 and 90 mm discs which are inserted into plastic or stainless steel housings specifically designed to accommodate the media height. Self-contained molded devices are also available. In both cases it is advantageous to use assemblies with integral air vents to avoid air entrapment and ensure complete utilization of the membrane area. These small-scale devices are important for process development studies with limited amounts of feed stream. Due to the variability in media, however, caution should be made in scaling up results obtained with such small filter areas. Some pilot scale devices are also available from certain manufacturers but there is no universal standard format at this scale. Industrial scale systems utilize stainless steel housings incorporating either 12 in. diameter (1.7–2.5 m²) or 16 in. diameter (3.4–5.0 m²) cartridges. Housing sizes range from 1 to 16 cartridges. Due to plant height limitations and safety concerns, housings are also available with split domes. Larger systems are often implemented with multiple housings in parallel (for capacity) and in series (for two-stage filtration to capture different particle sizes). In some cases the series configuration of housings can be avoided by using multimedia cartridges. There are, however, trade-offs to be made in terms of surface area per cartridge (which varies between manufacturer) and depth filter media height (some multimedia cartridges only contain half the media height for each filter).

Self-contained large-scale depth filters have also become available.

5.4. Processes

Cellulose depth filtration media pads are used in biotech processes for feed streams that cannot readily and cost-effectively be clarified with other types of filters. The most common application is using depth filtration downstream of either a centrifuge or tangential flow microfiltration system for protein harvest from fermenters. The combination of fibrillated cellulose and various filter aids combine to provide high capacity for challenging feed streams that include cell debris, DNA, protein aggregates, and colloidal material. Most cellulosic depth filters also contain a positively charged ligand that can significantly contribute to adsorption of negatively charged species and enhance the clarification process. The importance of electrostatic interactions can be tested by either running feed streams with increasing conductivity or by performing a high salt elution after loading the filter. Particle size and zeta potential data on the feed and eluate can provide insights into removal mechanisms.

Depth filters are also made from synthetic polymers in both neutral and charged versions, e.g., spun polypropylene fibers with a graded fiber size. These filters may be used in harvest applications although the cellulose filters have significantly higher frontal areas, process capacities, and clarifying ability. A more common application is as guard filters on chromatography columns. Benefits in such applications include high capacity for relatively pure protein feed streams. One downside is that they are not absolute 0.2 μm rated and hence do not provide protection against air accidentally entering the column. While high capacity sterile filters provide both clarification and protection against air, they are significantly more expensive.

6. Virus filtration

6.1. Principles

Virus filtration can provide a robust, size-based viral clearance mechanism that complements other virus clearance steps in the production of biotherapeutics [40]. Since the presence of only a small number of abnormally large pores will permit excessive virus leakage, virus filters must be manufactured so as to eliminate all macro-defects. This is typically accomplished through the use of composite membranes that provide the required combination of virus retention and mechanical stability. In addition, multiple layers of membrane are often used. Virus filtration membranes are made from hydrophilic polyethersulfone, hydrophilic polyvinylidene fluoride, and regenerated cellulose [41,42].

Virus filters were originally designed for use in tangential flow filtration (TFF) with the feed flowing adjacent to the upper skin layer of the asymmetric membrane [43]. TFF provides high flux by sweeping the membrane surface to reduce concentration polarization and fouling. However, the simplicity and lower capital cost of normal flow filtration (NFF) has led to the widespread use of virus filters specifically designed for NFF. In contrast to TFF, these normal flow filters are typically operated with the more open side of the membrane facing the feed stream [44], allowing protein aggregates and other large foulants to be captured within the macroporous substructure thereby protecting the virus-retentive skin layer. Single-use normal flow filters simplify both system design and validation, reducing labor and capital costs.

6.1.1. Virus retention

Virus retention is characterized in terms of the Log Reduction Value (LRV), which is defined as the logarithm (base 10) of the ratio of the viral concentration in the feed to that in the filtrate:

$$\mathrm{LRV} = -\log_{10}S \tag{9}$$

where S is the sieving coefficient for the virus. The total required LRV depends on the nature and potential for viral contamination of the starting material. Biologicals produced from cell lines containing retroviruses will typically require higher LRV. Virus filtration steps are typically designed to provide a minimum of 4-log virus removal. Viral clearance studies are performed by spiking high titer infectious viruses (with different physical characteristics) into scaled-down modules and evaluating the LRV. Removal of both enveloped and non-enveloped viruses must be demonstrated. Common model viruses include animal parvoviruses (e.g., MVM), poliovirus, SV40, sindbis virus, and reovirus. Retrovirus filters are designed to remove only larger viruses (greater than approximately 50 nm) while parvovirus filters are designed to provide significant removal of viruses as small as 20 nm. Initial design studies can also be performed with bacteriophages which can be obtained at much higher purity and titers, and which are much easier (and less expensive) to assay.

6.1.2. Fouling phenomena

Fouling during virus filtration is typically dominated by protein aggregates, DNA, partially denatured product, or other debris. This can be a significant problem in spiking studies since the virus preparations are often quite "dirty", with fouling characteristics that are very different than the actual process stream. Fouling can be significantly reduced using appropriate pre-filters [45]. Scale-up of virus filters is done using the same basic strategy as used for sterile filtration.

6.2. Membranes

6.2.1. Flat sheet

Millipore Corporation produces a number of skinned, composite flat sheet membranes specially manufactured to avoid formation of macrovoids. The first of these membranes were produced from hydrophilized PVDF and were designed to pass proteins with 70 or 180 kDa molecular weight: the Viresolve® 70 membrane and the Viresolve® 180 membrane, respectively [43]. The composite structure of these Viresolve® membranes features a thin, asymmetric, ultrafiltration layer cast on a microfiltration membrane. The pore size in the ultrafiltration layer increases gradually from the "skin" layer progressing towards

the large pore microfiltration layer. Viresolve® membranes are used in tangential filtration devices.

Pall Corporation has developed the Ultipor® DV50 and DV20 membranes [46] for normal flow virus filtration. The DV20 consist of two membrane layers while the DV50 has three membrane layers. Each membrane is made from a relatively homogeneous hydrophilized PVDF. The DV50 is designed to remove retroviruses (>50 nm) while the DV20 provides significant removal of the smaller parvoviruses.

More recently, Millipore introduced the Viresolve® NFP and NFR filters for normal flow filtration [44]. These are multilayer structures designed for parvovirus (NFP) and retrovirus (NFR) removal. The Viresolve® NFP is made from hydrophilized PVDF while the Viresolve® NFR is a hydrophilic polyether-sulfone in which the densest layer is in the interior of the membrane.

6.2.2. Hollow fiber

Asahi Kasei Corporation (Japan) manufactures 15N, 20N, and 35N Planova® hollow fiber membranes made from naturally hydrophilic cuprammonium regenerated cellulose [47,48]. The effective filtration layer is approximately 35 μm thick to assure high viral retention. The Planova filters were among the first membranes specifically designed for virus filtration, and numerous studies have explored the behavior of these membranes both for virus filtration [49] and for removal of pathogenic prion protein [50]. The Planova 35N membrane is capable of removing viruses larger than 35 nm in size while the 15N membrane provides a significant clearance of essentially all viruses. Hongo-Hirasaki et al. [51] have demonstrated that the Planova 20N provides high levels of porcine parvovirus removal from human IgG solutions with minimal fouling.

6.3. Modules

6.3.1. Tangential flow modules

Tangential flow filtration for virus removal is typically performed using hollow fiber modules or flat sheet cassettes. Hollow fiber cartridges use an array of narrow bore, self-supporting, fibers potted at the ends in an epoxy or polyurethane resin and housed within a cylindrical cartridge. Flat sheet cassettes typically employ a sandwich arrangement of a permeate screen, membrane, and retentate screen. The screens define the flow paths and increase mass transport in the polarization boundary layer.

6.3.2. Normal flow VF modules

Normal flow virus removal filters typically use pleated membranes in cartridge form. The membranes are supported on non-woven polyester, folded to form pleats, wrapped around an inner core, and sealed by the use of two end caps. Support cages are often placed around the membrane to protect it against mechanical damage. Cartridges are available in a variety of sizes (e.g., 10, 20, 30, and 40 in.). The cartridge is placed inside a stainless steel housing prior to use. Self-contained cartridges called

capsules are attractive since they do not require a housing and are easier to use. Smaller volumes can be processed with cartridges containing a stack of membrane discs.

6.4. Equipment

Virus filtration was originally performed exclusively using tangential flow filtration devices originally designed for ultrafiltration (see Section 8.3). Normal flow filtration cartridges are made using the Code 7 standard for corresponding stainless steel housings (see Section 3.3). Small-scale formats for process development, characterization, and validation studies include individual membranes (25–47 mm diameter) for use in stainless steel disc holders and self-contained devices. Pilot scale devices exist in both self-contained formats as well as in 1 in. versions of the standard Code 7 cartridges.

6.5. Processes

6.5.1. Protein capacity studies

Virus filters are divided into two categories. One category is used for clearance of large viruses such as retroviruses (approximately 100 nm diameter) using pore sizes in the range of approximately 50–70 nm. A second category includes filters designed to remove smaller viruses such as parvoviruses (as small as 22 nm diameter) using pores sizes of approximately 20 nm. Protein capacity studies for virus filtration applications follow the same principles as outlined for sterile filtration (see Section 3.5). It is important to perform development studies using the same pre-filter (if used), operating principles, and set points (constant flux or constant pressure). The feed stream must be representative of industrial scale processing including both storage time and storage temperature, both of which have a significant impact on process capacity. It is also important to extend the capacity study beyond the throughput in manufacturing (1.5–2 times) to deal with feed stream and membrane lot-to-lot variability. Process characterization studies may be performed to investigate process capacity and yield as a function of a range of process parameters.

6.5.2. Virus filtration validation studies

Virus filtration validation studies are performed at small scale typically using self-contained devices with 13–47 mm discs. All process parameters are scaled down in a linear fashion and should represent worst-case conditions with regard to virus clearance. It is also important to process a larger amount of feed stream per surface area compared with the industrial scale process design to insure validation under worst case process conditions. Virus clearance should be measured in several fractions. Several recent studies have demonstrated that virus clearance can decrease with the extent of membrane fouling (reduction in permeability) when using parvo-type virus filters (20 nm pore size) [52]. This effect has not been seen with retrovirus type filters (70 nm pore size). Depending on the overall process validation requirements one or more viruses may be studied to cover a range of particle sizes.

6.5.3. Industrial scale processes

Industrial scale processes typically use Code 7 cartridges and housings and utilize many of the same principles as sterile filtration. Sanitary operation ("closed processing") is maintained with either SIP or chemical sanitization (typically 0.1–0.5N NaOH) after assembly and prior to use. Pre-use integrity testing may be done to insure proper cartridge installation and/or to mitigate against risk of having to re-process the feed stream should the post-use integrity test fail. Post-use integrity testing is required to insure that the claimed virus clearance was in fact achieved since it is not feasible to determine the virus content in the filtrate at the low levels required for human pharmaceuticals produced from mammalian cells (<1 virus particle per million doses). The filter manufacturer must also correlate the integrity test parameters with virus clearance.

7. Membrane chromatography

7.1. Principles

7.1.1. General

Membrane chromatography uses microfiltration (or larger) pore size membranes that contain functional ligands attached to the inner pore surface throughout the membrane structure to provide highly selective separations through adsorption/binding interactions. Ion exchange, affinity, reversed-phase, and hydrophobic interaction membranes have been developed. Although the equilibrium binding capacity in membranes tends to be low, the convective flow through the pores reduces the mass transfer resistance compared to column (bead) chromatography. This can be particularly important for purification of large biomolecules and viruses that can have significant diffusion limitations in conventional chromatographic media. Membrane chromatography also has higher flow rates, lower pressure drops, and shorter processing times than conventional chromatography [53].

There has been significant interest in using membrane chromatography for bioprocessing for more than 20 years, but there have been few commercial successes. Binding capacities for membrane systems remain below those for conventional bead chromatography. Recent improvements in membrane materials and chemistries, coupled with a greater appreciation of appropriate target applications, have generated renewed interest in applications of membrane chromatography for bioprocessing.

7.1.2. Convection and diffusion

The convective flow through the pores significantly reduces the mass transfer resistance in membrane chromatography, with the dynamic binding capacity typically independent of the flow rate over a fairly large range of operating conditions. Suen and Etzel [54] developed a model for the effects of convection, diffusion, and adsorption, including the non-uniformity in the flow distribution.

7.1.3. Exclusion phenomena

Recent studies of ion exchange chromatography bead media have demonstrated the presence of exclusion phenomena that can reduce the mass transport rate of protein into beads [55]. The phenomenon occurs for large proteins such as monoclonal antibodies (160 kDa) using typical resin pore sizes. The effect appears to be due to initial binding of proteins at the pore entrance that results in steric hindrance and charge repulsion of subsequent protein entering the pore. The effect has also been observed for smaller proteins such as antigen binding fragments (44 kDa) for small pore size resins.

Studies of membrane chromatography have shown that the exclusion phenomenon also appears to exist with membrane media. Fig. 11 shows the normalized dynamic binding capacity (DBC/DBC$_{max}$) at 10% breakthrough ($C/C_0 = 0.1$) for a Pall Mustang®-S membrane and GE Healthcare Sepharose™ Fast Flow and Sepharose™ XL resins using the same monoclonal antibody at three different pH. Exclusion effects are greatest at pH 4 and low conductivity, conditions that lead to strong electrostatic interactions. The exclusion phenomenon has been directly observed in bead media using confocal microscopy [55]. No such direct evidence exists yet for membranes. Both types of media do, however, exhibit the same general trends with regard to DBC as a function of load conductivity. Since pores are used for convective flow through a membrane media, an exclusion phenomenon may exist due to either surface exclusion (flat binding surface) or pore exclusion from membrane surface modifications (various methods used to increase binding capacity). The coincident curves are likely due to similar ligand densities. Traditional ion exchange theory predicts that maximum DBC is obtained at the highest protein net charge and the lowest conductivity. The presence of the exclusion phenomenon generates a maximum DBC at an intermediate critical conductivity that depends on the protein net charge. The maximum DBC is independent of protein net charge within a wide range (35–108) [55].

7.2. Membranes

A variety of base membrane materials can be modified to generate adsorptive membranes. The Pall Mustang® Q and S membranes are flat sheet polyethersulfone that have been modified with quaternary amine and sulfonic acid functionalities. Sartobind® membranes from Sartorius are made from a stabilized regenerated cellulose. Zeng and Ruckenstein [56] have reviewed the different base materials and surface modification chemistries that can be used to generate chromatographic membranes.

7.3. Modules

7.3.1. Stacked sheet

The required bed height for a membrane chromatography unit is achieved by using multiple layers of membrane in series. This also provides more uniform flow distribution, with any "defects" in one layer compensated for by the flow through the subsequent layers. The simplest geometry is to use a stack of membranes, typically circular disks, placed one on top of each other.

7.3.2. Pleated

Pleated cartridges for membrane chromatography are similar to those used for normal flow filtration. The Mustang® mem-

(A)

(B)

(C)
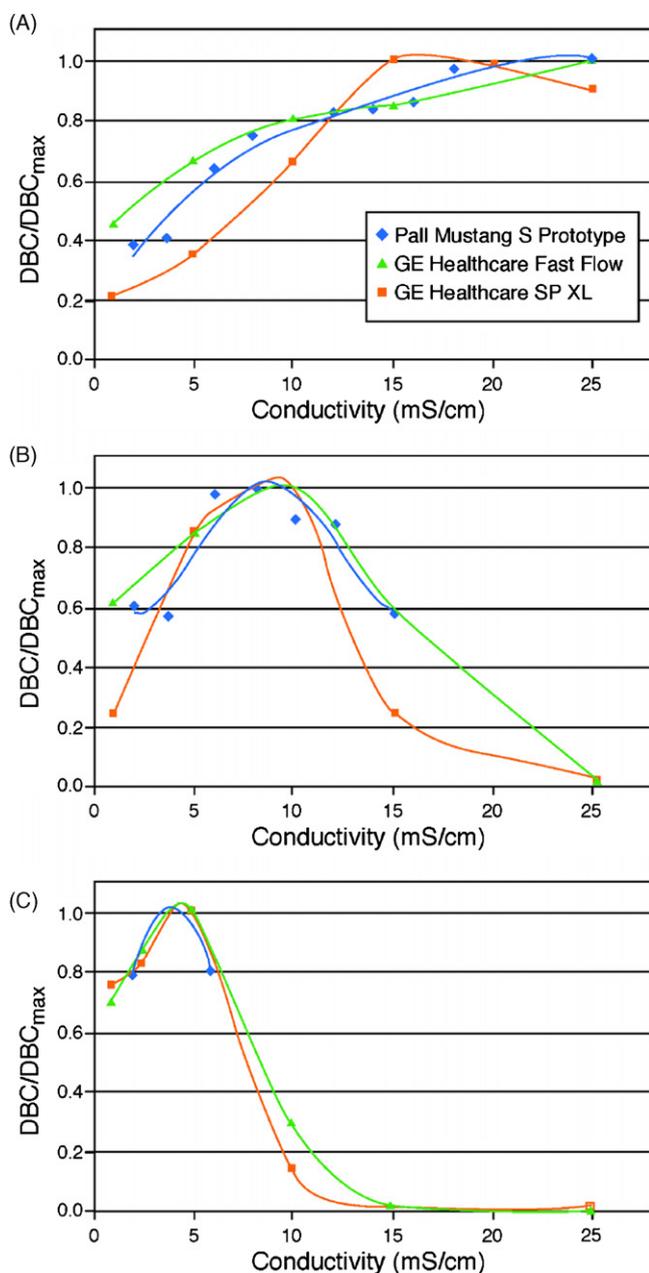
Fig. 11. Normalized dynamic binding capacity as a function of conductivity for two cation exchange resins (GE Healthcare Sepharose[TM] Fast Flow and Sepharose[TM] XL) and a cation exchange membrane (Pall Mustang® S prototype). Protein exclusion (charge repulsion) limits capacity at low conductivity [55]. Maximum capacities were 26 mg/mL for the membrane prototype and 70 mg/mL (Sepharose[TM] Fast Flow) and 100 mg/mL (Sepharose[TM] XL) for the resins. Panels are at: (A) pH 4, (B) pH 5, (C) pH 6. Data obtained by Ai P. Lin, Jay Mueller, Bénédicte Lebreton, Chithkala Harinarayan, and Robert van Reis at Genentech, Inc.

brane systems use a 16-layer pleat design. Process scale systems are now available with 5 L of membrane that can be operated at flow rates of 50 L/min (Fig. 12).

7.4. Equipment

Membrane chromatography modules are available with membrane media volumes ranging from 0.35 mL up to 5 L covering a range of flow rates from 3.5 mL/min up to 50 L/min

Fig. 12. Industrial scale membrane chromatography unit. Pall Mustang® 5 L XT 5000 module with 16 layers of pleated 0.8 µm PES membrane with quaternary amine ligand. Photo used with permission of Pall Corporation.

hence covering applications from laboratory to industrial scale. Modules exist as self-contained units or as modules that require insertion into stainless steel housings. Multiple modules can be connected together to achieve either higher flow rate or higher dynamic binding capacity or both.

7.5. Processes

7.5.1. Flow through applications

Membrane chromatography is emerging as an alternative to bead-based media for flow-through applications in which buffer conditions are set to enable binding of impurities while allowing product to flow through the media [53,57]. These applications can leverage the high linear velocities possible with membranes while maintaining the small media volumes generally required for binding small amounts of impurities in polishing steps. Removal of DNA, viruses, and endotoxins is typically comparable to bead based media whereas clearance of host cell proteins may require lower conductivities to achieve the same level of removal as bead-based media. Because of the small amount of media required for flow-through applications it is possible to use membrane chromatography units as single-use devices. This eliminates the need for re-use studies at small scale and for regeneration and sanitization at large scale.

7.5.2. Bind and elute applications

Membrane chromatography has also found use in bind-and-elute applications for large solutes such as DNA, RNA, and

viruses [58,59]. Most bead-based media have pore sizes that exclude very large solutes from entering the pores. The dynamic binding capacity in such media is therefore limited to the outer surface of the beads. Membrane chromatography provides competitive DBC for such applications. The larger internal surface area of beads combined with higher media packing densities has so far made it difficult for membranes to effectively compete on bind-and-elute applications for smaller solutes in terms of DBC, number of process cycles, and economics. It is likely, however, that such applications will become feasible with new developments in membrane structure and device design.

8. Ultrafiltration

8.1. Principles

Ultrafiltration is used for protein concentration and buffer exchange, largely replacing size exclusion chromatography for buffer exchange at industrial scale [60]. High protein retention is achieved by using a small pore size membrane, although recent studies have demonstrated the potential of exploiting both size and electrostatic interactions for enhanced ultrafiltration processes [9,61].

8.1.1. Permeability

The membrane permeability is typically evaluated from the water (or buffer) flux as a function of the transmembrane pressure based on Eq. (2). The analysis of data in tangential flow filtration devices is more complicated since the conversion of feed flow into filtrate creates a non-linear pressure drop on the retentate-side of the module. Accurate values of the permeability can be obtained by extrapolating a plot of $J/\Delta P$ versus ΔP to zero transmembrane pressure. The permeability is determined by the membrane pore size distribution, porosity, and thickness as well as the solvent properties. Low ionic strength solutions will give slightly lower permeability due to the effects of counter-electroosmosis associated with the non-zero streaming potential [8]. The measured permeability scales as the reciprocal of the solution viscosity, an effect that can be significant with concentrated solutions.

Membrane fouling reduces the process permeability compared to the clean membrane value. Process permeability for polysulfone membranes tend to be lower than those for regenerated cellulose due to the greater extent of protein adsorption on the more hydrophobic polysulfone [9].

8.1.2. Size exclusion

Protein retention in ultrafiltration has traditionally been viewed as a purely size-based exclusion phenomenon. The nominal molecular weight cut-off (MWCO) provides minimal information on product retention since membranes with the same MWCO but different pore size distributions can have very different behavior at the >99% retention level needed for ultrafiltration/diafiltration processes. The inherent trade-off between the hydraulic permeability and protein retention, using bovine serum albumin as a model protein, is shown in Fig. 13 [61]. The y-axis is simply the reciprocal of the protein sieving coefficient,
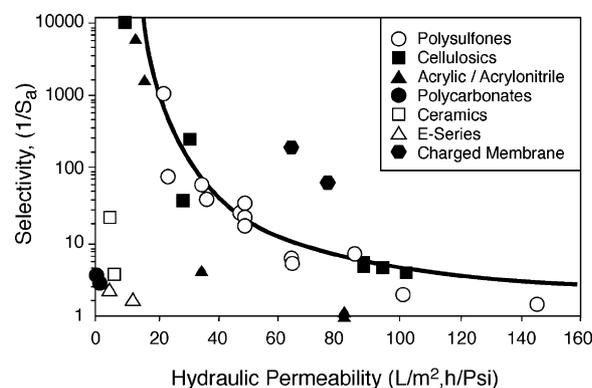
Fig. 13. Selectivity–permeability trade-off for ultrafiltration membranes using BSA as a model protein. The selectivity is defined as the reciprocal of the protein sieving coefficient. The solid curve is a model calculation accounting for steric interactions assuming a log-normal pore size distribution. Adapted from Mehta and Zydney [61].

which provides a measure of the selectivity of the membrane between a very small solute (sieving coefficient equal to one) and the protein of interest. The solid curve is a theoretical calculation accounting for purely size-based exclusion assuming a log-normal pore size distribution [61]. Most of the experimental data cluster along this theoretical curve, defining the "upper bound" for currently available commercial ultrafiltration membranes. The data points that lie well below the curve are primarily for track-etch membranes that have a lower porosity and greater thickness than the asymmetric ultrafiltration membranes.

8.1.3. Electrostatic exclusion

Charged proteins in an electrolyte solution are surrounded by a diffuse ion cloud or electrical double layer due to electrostatic interactions with the counter-ions and co-ions. Pujar and Zydney [15] have demonstrated that the effective size of the protein is increased by the presence of this diffuse electrical double layer. Additional electrostatic interactions arise from the increase in free energy associated with the distortion of the electrical double layer adjacent to the pore wall and from direct charge–charge interactions between the charged protein and charged groups on the membrane surface. These effects can be quite dramatic, with the sieving coefficient reduced by more than 100-fold due to a reduction in salt concentration from 100 to 1 mM [14].

The hexagonal symbols in Fig. 13 represent data obtained for a negatively-charged composite regenerated cellulose membrane produced by chemical attachment of a sulfonic acid functionality. This electrically charged membrane has much better performance characteristics (high permeability and high selectivity) than any of the commercially available membranes due to the strong electrostatic exclusion of the negatively-charged protein. These electrically-charged membranes can be used for enhanced ultrafiltration processes when the conductivity of the buffer solution is below 50 mS/cm.

8.1.4. Mass transfer

The filtrate flux in tangential flow ultrafiltration is typically governed by concentration polarization effects, which are com-

Table 2
Effect of buffer conditions on the mass transfer coefficient for a monoclonal antibody

pH	Protein net charge	Conductivity (mS/cm)	Mass transfer coefficient (L/m²/h)
6	33	1	73
6	33	20	49

High conductivity shields the charge on the protein thereby reducing the diffusion coefficient and in turn the mass transfer coefficient. Using a low pH and low conductivity buffer increases the mass transfer coefficient providing much higher ultrafiltration fluxes. Data obtained by Data obtained by Amy Len and Robert van Reis at Genentech, Inc.

monly described using the classical stagnant film model [5]:

$$J = k \ln \left(\frac{C_w - C_f}{C_b - C_f} \right) \tag{10}$$

where k is the protein mass transfer coefficient in the particular membrane module and C_w, C_b, and C_f are the protein concentrations at the membrane surface, in the bulk solution, and in the filtrate, respectively. The mass transfer coefficient is a function of the device geometry, hydrodynamics, and protein diffusion coefficient. The protein diffusion coefficient in turn depends on the protein charge (pI and pH), buffer conductivity, and protein concentration. These effects can be quite pronounced, with the mass transfer coefficient varying by as much as a factor of two in different buffers due to the differences in protein charge and intermolecular electrostatic interactions (Table 2). The diffusion coefficient is also proportional to the absolute temperature and inversely proportional to the viscosity, which itself is a strong function of temperature. This can result in large increases in mass transfer coefficient and hence filtrate flux at higher operating temperatures as shown in Fig. 14.

The mass transfer coefficient can be experimentally determined as described in Section 8.3. In addition, mass transfer coefficients and channel pressure differentials can be calculated as follows:

$$k = \beta * Q \tag{11}$$

$$\Delta P = \text{constant} * Q^\alpha \tag{12}$$

where $\alpha = 1$ for laminar flow, $\alpha = 1–2$ for transition zone (typical value for screened channel is $\alpha = 1.3$) and $\alpha = 2$ for fully turbulent flow. Eq. (11) is approximate and is valid only over a limited range of feed flow rates. The parameter β is a function of the detailed geometry of the screen. Typical data are shown in Fig. 15, with the mass transfer coefficients at high feed flow rates differing by as much as a factor of three. It should be noted that at constant feed flow rate and high conversion ratios (filtrate rate/feed flow rate) the mass transfer coefficient will decrease along the length of the module due to the reduction in the local retentate flow rate.

The protein concentration at the membrane surface increases with increasing filtrate flux, which may result in an increase in protein transmission. In addition, the osmotic pressure increases thereby reducing the effective pressure driving force for filtration. Since the osmotic pressure of a concentrated protein
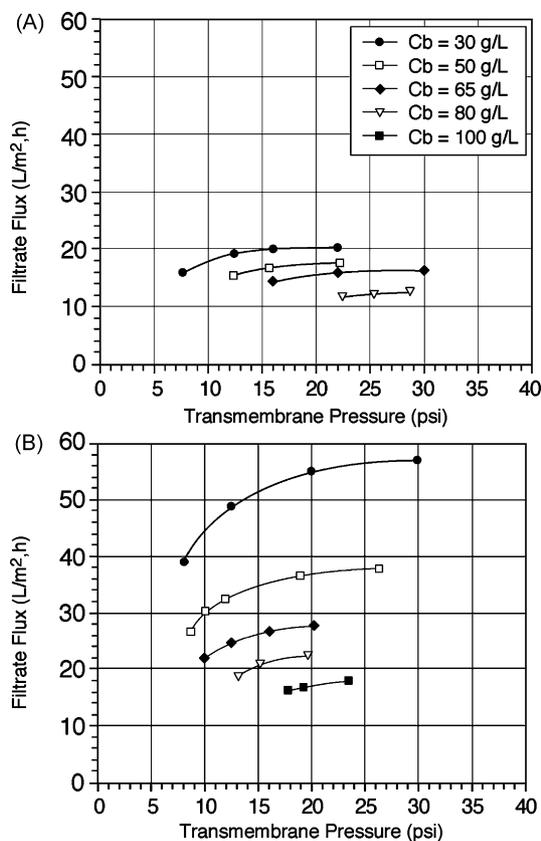
Fig. 14. Ultrafiltration flux for a monoclonal antibody in a 50 mM histidine buffer with a 30 kDa composite regenerated cellulose membrane at 23 °C (A) and 37 °C (B). The flux increases by almost three-fold due to the mass transfer coefficient being proportional to the diffusion coefficient to the 2/3 power and the diffusion coefficient being proportional to the absolute temperature and inversely proportional to the viscosity [6]. The viscosity was decreased four to five-fold by increasing the temperature. Data obtained by Charles Winter at Genentech, Inc.
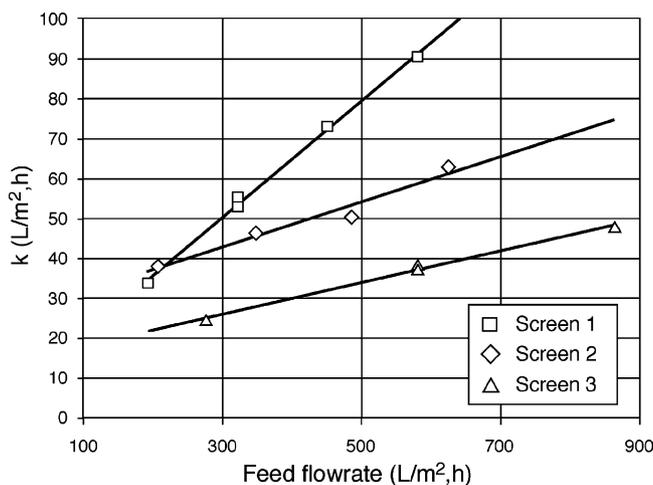
Fig. 15. Protein mass transfer coefficients for a monoclonal antibody as a function of area-normalized feed flow rate for UF cassettes with three different retentate screens. Data obtained by Aaron Pruett, Poonam Mulherkar, and Robert van Reis at Genentech, Inc.

solution has a highly non-linear dependence on the protein concentration [62], the transmembrane pressure increases dramatically when the flux approaches a critical value, which is typically referred to as the pressure-independent flux. High protein concentrations can also reduce the membrane permeability through irreversible fouling or through the formation of a protein gel or cake on the membrane surface. In this case, the pressure-independent flux is determined by the protein solubility or gel concentration.

8.2. Membranes

8.2.1. Flat sheet

Flat sheet ultrafiltration membranes are cast from a variety of polymers, including polysulfone, polyethersulfone, and regenerated cellulose. These membranes have an asymmetric (skinned) structure, with the thin skin providing the desired selectivity while the more porous substructure provides the necessary mechanical support. Synthetic polymers have high thermal stability and chemical resistance, allowing the use of fairly harsh cleaning chemicals. Regenerated cellulose membranes (Fig. 16A) are more hydrophilic, reducing both protein adsorption and fouling. New composite regenerated cellulose membranes (Fig. 16B) have excellent mechanical strength and cause very little fouling, providing higher flux and better retention characteristics than other membrane chemistries [9].

8.2.2. Hollow fiber

Hollow fiber ultrafiltration membranes are made from similar polymers as their flat sheet counterparts. These membranes are self-supporting, so they can be cleaned by backflushing. Hollow fiber devices do not need spacers or multiple sealing procedures, which reduces labor costs involved in assembly, but the lack of spacers typically results in somewhat lower mass transfer coefficients. Fiber breakage can also be a problem, thus it is critical to follow the manufacturer's recommendations with respect to operating pressures.

8.3. Modules

Hollow fiber, flat-sheet cassettes, spiral wound cartridges, tubular modules, and enhanced mass transfer devices have all been developed for ultrafiltration. These modules provide physical separation of the retentate and filtrate streams, mechanical support for the membrane (if needed), high membrane packing densities (membrane area per device volume), easy access for cleaning and replacement, and good mass transfer characteristics. Spiral wound modules are subject to plugging, are more difficult to clean, and have a more limited range of scalability than hollow fiber modules or flat-sheet cassettes. Rotating and Dean vortex systems have also been developed for ultrafiltration. These devices have high mass transfer coefficients but lower packing densities [63], and they can be difficult to scale-up (or down) due to changes in hydrodynamic conditions [9].

8.3.1. Linear scale cassettes

The most effective approach to scale-up of ultrafiltration devices is linear scaling in which the pressure, fluid flow, and
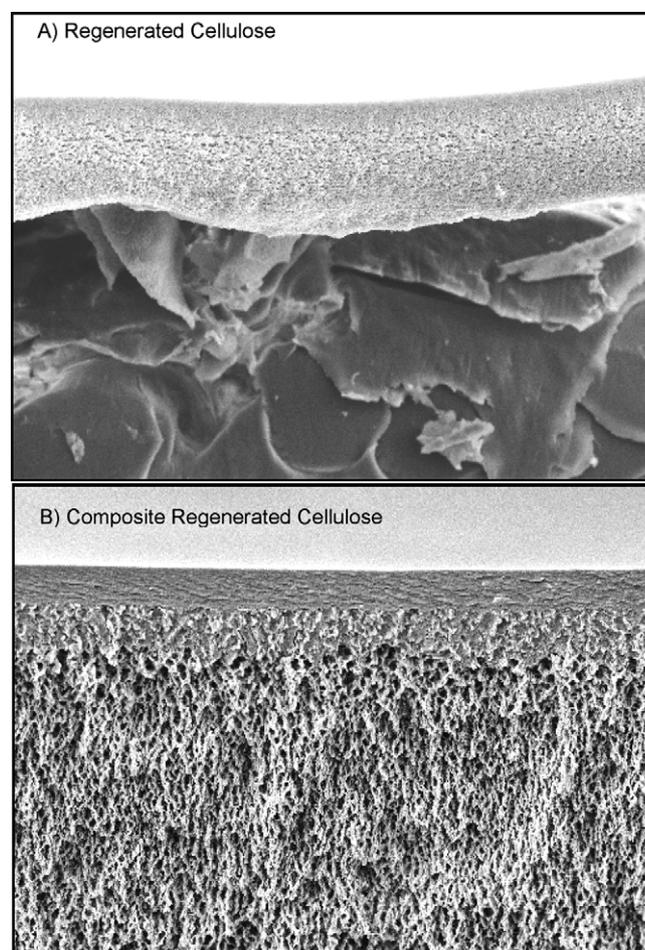
Fig. 16. (A) Regenerated cellulose membrane provides very low fouling (0–20%) chemistry for ultrafiltration membranes with complete cleaning (100% of original permeability) using 0.1N NaOH at ambient temperature). (B) Composite regenerated cellulose also provides defect-free active layer with robust bond between the cellulose ultrafiltration layer and the polyethylene microporous substrate to prevent delamination due to inadvertent reverse pressure spikes. Scanning electron micrographs used with permission of Millipore Corporation.

concentration profiles along the length of the filtration module remain constant when changing scale of operation [64]. Linear scaling can only be achieved by keeping the channel length constant, with the area changed by increasing (or decreasing) the number of fibers or parallel channels. It is also possible to change the channel width in flat-sheet cassettes, although some care must be taken to ensure uniform flow distribution. Equal flow distribution among channels (or fibers) is achieved using appropriate piping manifolds and proper design of entrance and exit regions. Linear scale flat-sheet cassettes have been developed specifically for bioprocessing applications that provide 1000-fold scaling of ultrafiltration processes with consistent product yield and process flux [64]. Recent developments include automated manufacturing of robust third generation thermoplastic cassettes covering a range of linear scale modules from $100 \, cm^2$ to $1 \, m^2$ with built-in gaskets, tight tolerances for pressure drop, reduced parasitic pressure losses, and high pressure capability (up to 7×10^5 Pa (7 bar)) as shown in Fig. 17.

Fig. 17. Linear scale ultrafiltration cassettes with constant channel length and mass transfer coefficient (same turbulence promoting screen and channel compression) can provide thousand-fold linear scale-up of ultrafiltration processes. Twenty-thousand-fold linear scale-up is possible with new linear scale devices such as Millipore Pellicon® 3 cassette. Photo used with permission of Millipore Corporation.

8.4. Equipment

Large-scale ultrafiltration systems used in biotechnology were originally based on equipment used in the food and dairy industries. This equipment posed several significant limitations. Sanitary design was not suitable for processing of human pharmaceuticals, cleaning procedures were cumbersome, and the systems lacked the ability for linear scaling (see previous section). Polysulfone membranes were mechanically robust but easily fouled and were difficult to clean. Cellulose membranes were low fouling and easy to clean but were very prone to delamination with costly yield losses and plant down-time. All of these issues were resolved by: (1) developing mechanically robust composite regenerated cellulose membranes (Fig. 16B), (2) introducing simple and effective sanitizing (peroxyacetic acid) and storage solutions (0.1N NaOH), and (3) developing linear scale-down and scale-up versions of the modules. Housing design was converted from a horizontal to a vertical design, alignment rods were introduced to avoid offsets between cassettes, internal bores were increased to match processing flow rates, and ports were redesigned to adapt to industrial piping designs.

The advent of high dose products (>100 mg/mL protein concentrations) with annual metric ton production requirements has led to the development of larger housings (up to 4 in. internal bore with a 6 high holder design and 10 cassettes per side), larger systems (6 in. pipe and 2800 ft^2 surface area) and low hold-up volume designs (total minimum operating volumes down to 66 mL/ft^2). A low hold-up volume design was achieved using several new design concepts (Fig. 18). The recycle tank was re-

Fig. 18. High concentration UF system with 250 m^2 membrane area. New tank design with a retentate lift tube combined with close-coupling of all feed and retentate components in a vertical arrangement resulted in a minimum operating volume (including product in the recycle tank) while maintaining good mixing, minimal short-circuiting of retentate to feed, and no air entrainment. Photo used with permission of Genentech, Inc. and Millipore Corporation.

designed so that it consists of a cylinder and cone with the height of the cylinder and the height of the cone equal to the radius of the cylinder. The outlet of the tank is at the bottom of the cone as in conventional tank design but the retentate tube enters through the bottom of the cone, instead of the traditional dip-tube design which normally enters through either the top or side of the cylinder, thereby minimizing hold-up volume. The retentate tube has a tee outlet instead of straight pipe. This aids in good mixing within the tank without short-circuiting back into the tank outlet and without air entrainment at low operating volumes. The mixer location, angle, and rotation (up-pumping instead of down-pumping) were optimized using pilot and full scale mixing studies to ensure good mixing during concentration and diafiltration. The mixer is not used during final concentration. Feed and retentate piping were minimized by close-coupling all components in a vertical design. The tank outlet valve was connected directly to the feed pump via a 90° elbow (to facilitate pump maintenance). The pump was connected directly to a flow meter, cross (pressure switch and sample valve) and isolation valve mounted directly on the top of the cassette holder. Conventional designs have the feed entering through the bottom of
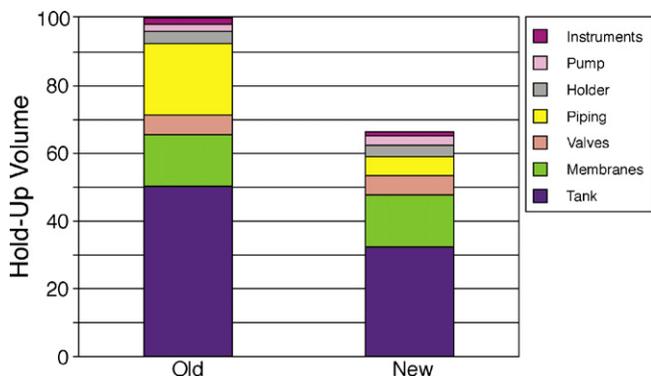
Fig. 19. Hold-up volume for old and new UF systems. The y-axis is on a relative scale with 100 corresponding to the total volume of the old UF system. Data obtained by Leah Frautschy, Chris Dowd, Doug Harris, and Robert van Reis at Genentech Inc. and Aline Kurljian and Elizabeth Goodrich at Millipore Corporation.

the holder, which adds a significant amount of pipe. Priming of the vertical pipe design was verified, and air entrainment was eliminated, using buffer prior to introduction of protein into the system. Pressure transducers for feed, retentate, and filtrate were located directly on the holder. The need for long pipe lengths before and after the flow meter were eliminated by recognizing that the application only required accuracy at 50–100% of the flow rate range. The cassette holder was used as part of the recycle loop and the retentate line included only the holder isolation valve, product transfer/buffer addition valve, tank isolation valve with integrity test nitrogen valve, and a short pipe section to match the height of the feed line components. Upper and lower filtrate valves were used for process and drain phases, respectively. A product recovery valve was located on the bottom of the holder further eliminating pipe (normally inserted into recycle loop) and improving product recovery. Product recovery is accomplished by buffer displacement in a completely vertical design with lower density buffer chasing higher density protein solution. Fig. 19 shows the distribution of hold-up volume compared with a conventional design. The new system has one-third less hold-up volume, with the most significant reductions in the tank and piping.

8.5. Process configurations and diafiltration

Ultrafiltration processes are typically carried out as a Fed Batch operation (Fig. 20A) if large concentration factors are required, followed by Batch operation (Fig. 20B). If buffer exchange is required this is typically carried out as a constant retentate level diafiltration operation (Fig. 20C). Diafiltration is performed at an optimum bulk concentration. Final concentration is then performed in batch mode.

The concentration of solutes during constant volume diafiltration is given by:

$$C = C_0 e^{-SN} \tag{13}$$

where C is the solute concentration, C_0 is the initial concentration of the solute, S is the sieving coefficient for the solute, and N is the number of diavolumes (buffer volume divided by retentate
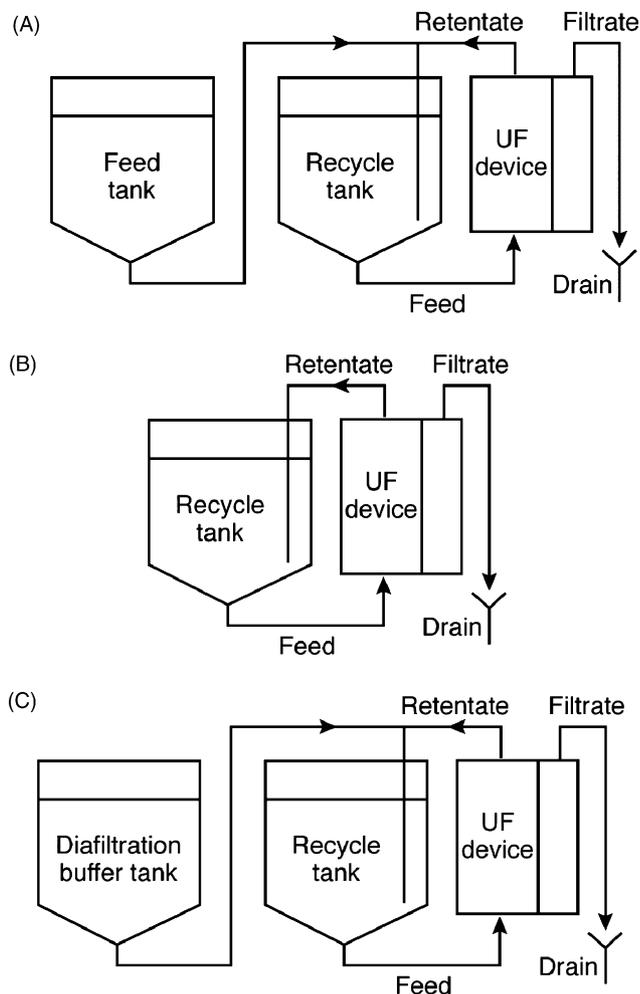
Fig. 20. (A) Fed Batch ultrafiltration operation for a retained product. (B) Batch ultrafiltration operation for a retained product. (C) Diafiltration operation for a retained product.

volume). Sieving of even very small solutes may not equal unity due to Donnan effects or due to inclusion in detergent micelles (if used). Clearance of small molecules may not follow the theoretically predicted value even when sieving is unity. An example is shown in Figs. 21 and 22 where citrate clearance was reduced due to equilibrium binding to a retained protein. This effect was not seen with HEPES or TRIS.

8.6. Process optimization and control

Ultrafiltration has traditionally been operated using either constant retentate pressure or constant transmembrane pressure with either manual or automated systems. Both methods provide simple process control. Process optimization has traditionally been accomplished by empirical investigation of feed flow rate, retentate (or transmembrane) pressure, and diafiltration bulk concentration. Equations for mass transfer as a function of feed flow rate have been developed for several feed channel geometries and can be used to aid in optimization of the feed flow rate.

Increasing mass transfer with either feed flow rate or through the use of turbulence promoters (feed channel screens) also
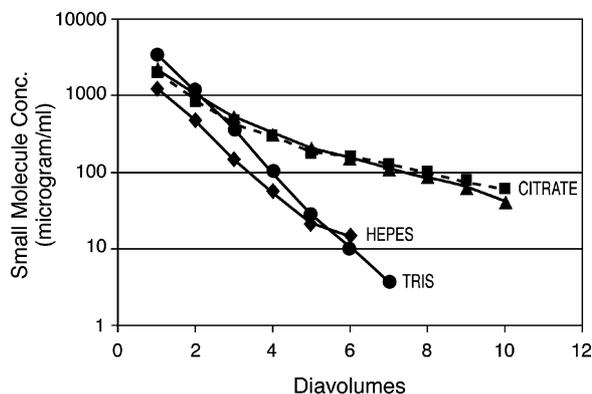
Fig. 21. Clearance of small molecules from a 48 kDa antigen binding fragment protein. Clearance of the multivalent citrate ion (filled squares and triangles) is reduced due to equilibrium binding to the protein. Diavolume denotes ratio of buffer volume added (equal to filtrate volume removed) to total retentate volume. Penultimate buffer with pH 6.2 and conductivity = 1.5 mS/cm and diafiltration buffer with pH 5.5 and conductivity = 0.7 mS/cm. Data obtained by Chithkala Harinarayan and Robert van Reis at Genentech, Inc.

leads to increased channel pressure drop which must be taken into account in the overall process design. Systematic studies of the effect of different screens and screen orientation have contributed to the optimization of screened channel UF devices [65,66].

Ng et al. [67] demonstrated that the stagnant film model predicts an optimum bulk concentration for diafiltration:

$$C_b^* = \frac{C_w}{e} \tag{14}$$

where C_b^* is the optimum bulk concentration for diafiltration (minimizing either process time or membrane area for a given number of diavolumes), C_w is the solute concentration at the membrane wall, and e is the natural logarithm base. Since C_w is not a priori known one must perform empirical studies of flux as a function of bulk concentration and determine the trade-off between flux and diafiltration volume.
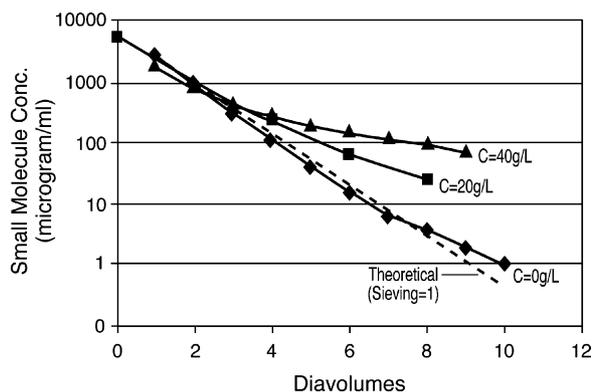
Fig. 22. Clearance of citrate ions from a 48 kDa antigen binding fragment protein solution is protein concentration dependent due to ion-protein equilibrium binding. The diafiltration process was improved by replacing the citrate (multivalent) buffer in the previous chromatography step with an acetate (monovalent) buffer which did not exhibit any binding to the protein. Diavolume denotes ratio of buffer volume added (equal to filtrate volume removed) to total retentate volume. Data obtained by Chithkala Harinarayan and Robert van Reis at Genentech, Inc.

From this it also follows that the optimal flux during diafiltration [9] is:

$$J^* = k \tag{15}$$

where k is the mass transfer coefficient. Recent studies have extended this analysis to include the effects of solute binding to the product on the optimal bulk concentration and flux [68].

An alternate method of process control using constant Cwall has been developed and implemented at industrial scale [69]. Cwall control provides more robust operation with better reproducibility, higher product yields, and larger operating flux compared to conventional constant pressure operation. By determining the mass transfer coefficient, osmotic virial coefficients, and fouled membrane resistance it is possible to optimize the ultrafiltration process without extensive empirical studies. The effect of changing process or plant parameters can readily be modeled without additional experimentation. Constant Cwall methodology can also be used to limit the maximum protein concentration at the wall to avoid exceeding solubility limits and guard against protein aggregation.

Several recent developments in Cwall methodology have led to improvements in both parameter determination as well as process control. The initial methodology used a step-wise determination of fouled membrane permeability (experimental), osmotic virial coefficients (fitting flux and transmembrane pressure data at several bulk concentrations to the osmotic pressure model), and determination of the mass transfer coefficient (also from fitting flux versus pressure data). The methodology was subsequently automated by fitting all of the parameters to the combined stagnant film and osmotic pressure models using flux versus transmembrane pressure data sets obtained at multiple bulk concentrations. A significant improvement in parameter accuracy was obtained with two modifications to the methodology. Direct measurement of both osmotic pressure virial coefficients and fouled membrane permeability reduced the inherent errors associated with fitting multiple parameters to the mathematical model.

A more fundamental change resulted from a revised evaluation of protein concentration polarization. A significant body of literature exists that explores mathematical models [5,70], physical interpretation of experimental data [6], and a limited amount of direct measurements of concentration polarization [71,72]. The presence or absence of a limiting concentration ("gel") has been explored mostly from the perspective of interpreting mathematical models based on predictions of filtrate flux data. Recent data on monoclonal antibodies supports a limiting concentration that depends on protein net charge and buffer pH and conductivity albeit without direct spectrophotometric evidence. Initial Cwall methodology used flux versus transmembrane pressure data sets in the pressure-dependent regime to avoid any potential changes in fouled membrane permeability. A limiting flux in the pressure-independent regime is, however, consistent with a limiting Cwall concentration. This is turn should result in a limiting fouled membrane resistance. Regardless of the physical phenomena, a limiting flux can be used to determine the mass transfer coefficient as the absolute value of the slope of
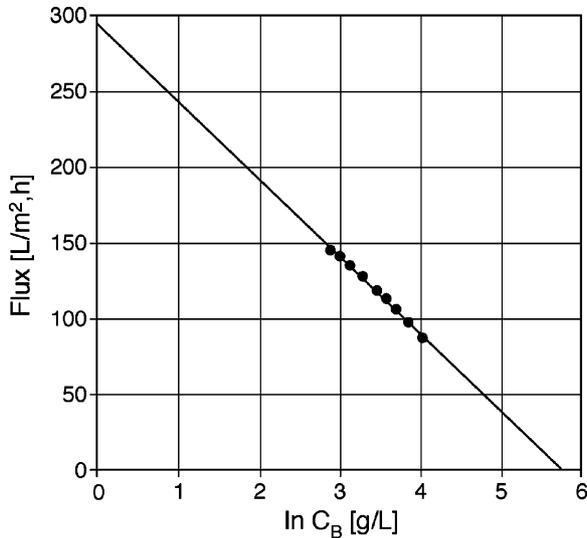
Fig. 23. Filtrate flux as a function of the logarithm of the bulk protein concentration in the pressure-independent regime. The slope provides a measure of the mass transfer coefficient and the zero-flux intercept gives the maximum Cwall for the given buffer. Data obtained with a monoclonal antibody at pH 4.9 (protein net charge = 58 based on amino acid sequence) and a buffer conductivity of 3.5 mS/cm using a Millipore Pellicon 3 Micro device (88 cm^2) at a feed flow rate of 324 L/m^2 h. Data obtained by Khoi Thai, Nuno Fontes, and Robert van Reis at Genentech, Inc.

flux versus the logarithm of the bulk concentration as shown in Fig. 23. The flux = 0 intercept of this line also provides the maximum Cwall that is achieved in the pressure-independent part of the flux versus TMP curve.

Fig. 24 shows a plot of the required membrane area and the required diafiltration buffer volume as a function of the bulk protein concentration at which the diafiltration is performed.
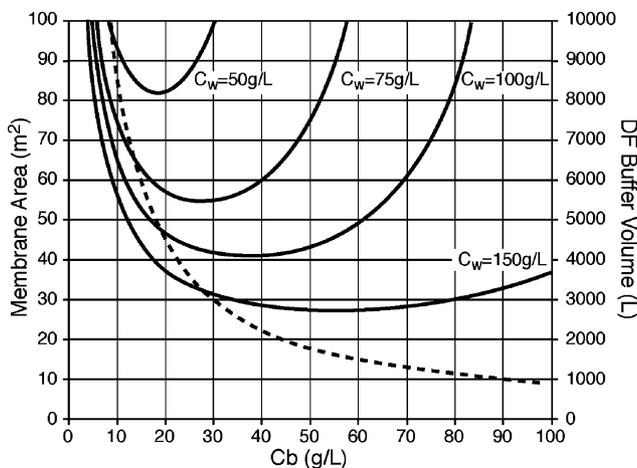
Fig. 24. Optimization of bulk concentration and buffer consumption for a 2-h diafiltration process with $C_0 = 3$ g/L, $V_0 = 3000$ L, $k = 30$ L/m^2 h and 10 diavolumes. Curves represent model calculations with different wall concentrations. The data are based on a monoclonal antibody with a penultimate buffer pH of 8 and conductivity of 7 mS/cm and a diafiltration buffer with pH 6.5 and conductivity of 20 mS/cm. Due to high conductivity the mass transfer coefficients were 30 L/m^2 h for both buffers. Higher C_w values provide a broader optimum and increased ability to reduce membrane area and diafiltration buffer volume (dashed line). Data obtained by Amy Len, Chithkala Harinarayan, and Robert van Reis at Genentech, Inc.

Calculations were performed for a fixed process time and number of diavolumes, corresponding to a fixed degree of small molecule clearance. Increasing C_b initially reduces the membrane area since less buffer volume is needed to achieve the same impurity removal. Very high bulk concentrations lead to an increase in membrane area due to the reduction in flux. The optimum C_b^* range, corresponding to the minimum membrane area, is wider at higher C_w values. Higher C_w also provides greater flexibility for a trade-off between membrane area and buffer consumption. Practical limits of minimum and maximum retentate volume, buffer tank size, UF system size, and membrane and buffer cost must also be taken into account.

The mass transfer coefficient depends on a number of parameters as outlined in Section 8.1. In general, mass transfer coefficients for proteins increase at lower buffer conductivity and as the absolute difference between pH and pI increases. This is due to an increase in diffusion coefficient with increased net charge. The charge effect is mitigated by charge shielding at higher conductivity. Mass transfer coefficients for monoclonal antibody monomers typically range from 30 to 55 L/m^2/h as shown in Table 2.

Extensive experience has demonstrated that protein aggregation in UF systems is primarily due to protein–oxygen interfaces caused by micro-cavitation in pumps and valves. Nitrogen-sparged solutions and nitrogen overlay virtually eliminates protein aggregation. Nitrogen overlay can also be used to control retentate pressure instead of a retentate control valve but operator safety must be considered (oxygen deprivation when opening large tanks with gas overlay). In practice, the amount of insoluble protein aggregates generated during UF is insignificant with respect to process yield. Turbidity of ultrafiltered protein solutions may still be high due to the dependence of scattered light on particle size. Fortunately, sterile filters provide an excellent means for removal of insoluble protein aggregates. While the amount of insoluble aggregates represents an insignificant amount of the total protein mass these feed steams do require a fair amount of sterile filter surface area for processing. The development of new high capacity sterile filters aid in such processes (see Section 3.2). Experience with a large number of monoclonal antibodies demonstrates that generation of soluble multimers in UF is generally not an issue, with the measured multimer content before and after UF often within the accuracy of the assay (fractions of a percent).

9. High performance tangential flow filtration

9.1. Principles

High performance tangential flow filtration is an emerging technology that uses semipermeable membranes for the separation of proteins without limit to their relative size [73,74]. This is in sharp contrast to conventional ultrafiltration processes that are generally thought to require a 10-fold difference in size for effective separation. HPTFF has been used to separate monomers from oligomers based on their difference in size [73], protein variants differing at only a single amino acid residue [75], and an antigen binding fragment from a similar
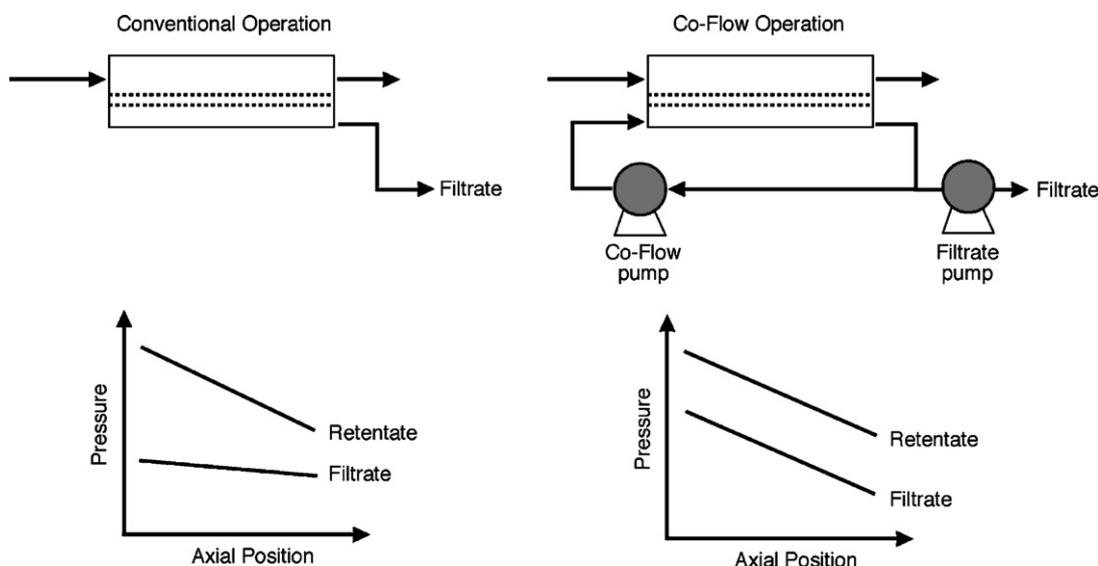
Fig. 25. Comparison of flow and pressure profiles for conventional TFF module and a module using co-flow arrangement to maintain a uniform transmembrane pressure throughout the module.

size impurity [7]. HPTFF can potentially be used throughout the purification process to remove specific impurities (e.g., proteins, DNA, or endotoxins) and/or eliminate protein oligomers or degradation products. In addition, HPTFF can effect simultaneous purification, concentration, and buffer exchange, providing an opportunity to combine several different separation steps into a single scalable unit operation. The high selectivity in HPTFF processes is obtained by exploiting a number of different phenomena as described in the following sub-sections.

9.1.1. Flux-TMP regime

As originally described by van Reis [76], HPTFF provides high selectivity by operating in the pressure-dependent regime at or below the "transition point" in a plot of filtrate flux versus transmembrane pressure. This minimizes fouling and exploits the effects of concentration polarization to increase the selectivity compared to that seen in the pressure-independent regime.

9.1.2. Co-current flow

Since the selectivity in HPTFF is a function of the local filtrate flux, and thus the local transmembrane pressure, the selectivity can be further improved by maintaining a nearly uniform transmembrane pressure throughout the module. Conventional membrane modules typically have a large variation in transmembrane pressure drop due to the parasitic pressure losses associated with flow along the retentate channel. A simple approach for minimizing this transmembrane pressure variation is to establish a co-current flow on the filtrate side of the membrane by using a recirculation pump to generate a pressure gradient in the filtrate channel that balances the gradient in the retentate (Fig. 25). Experimental data demonstrating the effect of co-current filtrate flow is shown in Fig. 26A and B. The selectivity, defined as the ratio of the sieving coefficient for the impurity to that of the product, is 10-fold larger when using co-current flow.

9.1.3. Buffer effects

A series of studies by Zydney and co-workers demonstrated that significant improvements in performance could be obtained by controlling buffer pH and ionic strength to maximize differences in the effective volume of the product and impurities [15,74,77]. As discussed previously, the effective volume of a charged protein accounts for the presence of a diffuse electrical double layer surrounding the protein [15]. Increasing the protein charge, or reducing the solution ionic strength, increases the effective volume thus reducing protein transmission through the
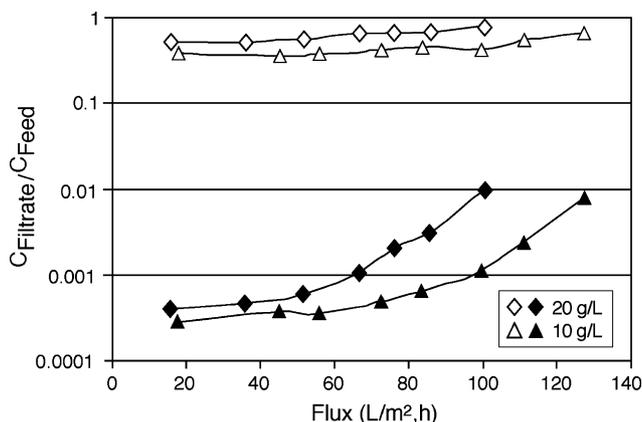
Fig. 26. (A) Sieving of a 20 mg/mL monoclonal antibody solution with Chinese hamster ovary protein (CHOP) impurities as a function of flux at pH 5 and pH 7 without co-current filtrate flow. Data obtained by Ailen Sanchez, Vassia Tegoulia, and Robert van Reis at Genentech, Inc. (B) Sieving of a 20 mg/mL monoclonal antibody (MAb) (closed symbols) solution with Chinese hamster ovary protein impurities (open symbols) as a function of flux at pH 5 and pH 7 with co-current filtrate flow. MAb sieving is reduced by more than 10-fold by using co-current filtrate flow while CHOP sieving remains high. The higher resolution separation is obtained by generating an even flux profile along the length of the filtration module thereby operating the entire membrane at an optimum flux. An alternate method of improving the flux profile is to reduce the permeability of the membrane without changing the pore size distribution. Data obtained by Ailen Sanchez, Vassia Tegoulia, and Robert van Reis at Genentech, Inc.

membrane. Optimal performance is typically attained by operating close to the isoelectric point (p*I*) of the lower molecular weight protein and at relatively low salt concentrations (around 10 mM ionic strength) to maximize electrostatic exclusion of the more retained species [74].

9.1.4. Membrane charge

Direct charge effects can be further exploited by using a membrane that has an electrical charge to increase the retention of all species with like-polarity. Thus, a positively charged membrane will provide much greater retention of a positively charged protein than will a negatively charged or neutral membrane of the same pore size [8]. Note that it may be possible to exploit electrostatic interactions even for solutes with identical p*I* due to the different charge–pH profiles for the different species and the combined effects of protein charge and size on protein transmission through the membrane.

9.1.5. Membrane pore size distribution

The membrane pore size distribution affects the selectivity by altering the solute sieving coefficients and the filtrate flow distribution. Theoretical calculations have demonstrated that elimination of large defects and reductions in the breadth of the pore size distribution can significantly improve the performance of HPTFF processes. However, the use of charged membranes provides an additional robustness to the process that would not be obtained using neutral membranes, lessening the importance of the pore size distribution. Future improvements in HPTFF technology will likely be focused on controlling the pore size distribution in electrically-charged membranes.

9.2. Membranes

Although a variety of membrane polymers and geometries could potentially be used for HPTFF, most of the work to date has focused on the use of flat sheet composite regenerated cellulose membranes that have been surface-modified to covalently attach either quaternary amine or sulfonic acid groups to provide the desired positive or negative charge, respectively. These membrane have excellent mechanical strength, cause little fouling, and provide high selectivity by exploiting both size and charge effects.

9.3. Modules

Membrane cassettes for HPTFF are similar to those used in ultrafiltration. Modules are specifically designed to provide linear scaling from very small modules suitable for process development ($A < 50\,\text{cm}^2$) to large commercial scale devices capable of processing 15,000 L in 3 h. HPTFF modules are used with a special holder that provides access to filtrate ports at both ends of the module to achieve the desired co-current flow.

9.4. Equipment

HPTFF uses the same equipment that has been installed in numerous small and industrial scale ultrafiltration systems (see
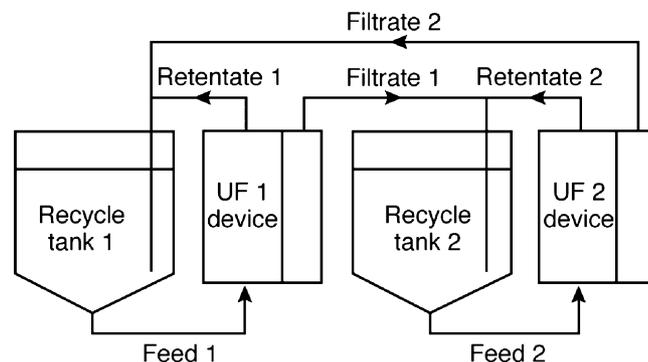
Fig. 27. Closed-loop two stage HPTFF system. Product in the first stage filtrate is continuously concentrated in the second stage while filtrate from the second stage is recycled and used as diafiltration buffer in the first stage.

Section 8.4). If co-current filtrate flow is required this can be accomplished by the addition of a co-flow loop and pump on the filtrate side. Some ultrafiltration cassette holders also require an adapter plate to separate the inlet and outlet filtrate streams. The hold-up volume associated with the co-flow loop should be minimized to reduce mixing of filtrate and filtrate recycle streams if it is desirable to track impurity levels in the filtrate.

9.5. Processes

9.5.1. Single stage

The most common application of HPTFF involves single stage systems in which the product is retained by the membrane while impurities pass through. These systems are completely analogous to conventional UF systems with the possible addition of a filtrate co-flow loop (Fig. 25).

9.5.2. Cascades

Two-stage cascade systems may be used when the product is in the filtrate. An example of a closed-loop two-stage HPTFF system is shown in Fig. 27. An example of a process using a two-stage HPTFF system is purification of albumin monomer from multimers. Albumin monomer passes through the first stage membrane while multimers are retained. The second stage membrane retains the monomer and filtrate is recycled (closed-loop) back to the first stage recycle tank and used as the diafiltration buffer thereby drastically reducing buffer consumption. Cheang and Zydney [78] also used a two-state HPTFF process to purify β-lactoglobulin and α-lactalbumin from whey protein isolate.

9.5.3. Process optimization

9.5.3.1. Optimization equations.
HPTFF is optimized by determining the best trade-off between yield and purity while minimizing membrane area and buffer consumption and maintaining an acceptable process time. A set of optimization equations (and/or diagrams) have been developed [79] that relate all of these parameters to the selectivity and mass throughput for a product collected in the retentate:

$$P_R = Y_R^{1-\psi} = \exp(N\,\Delta S) \tag{16}$$
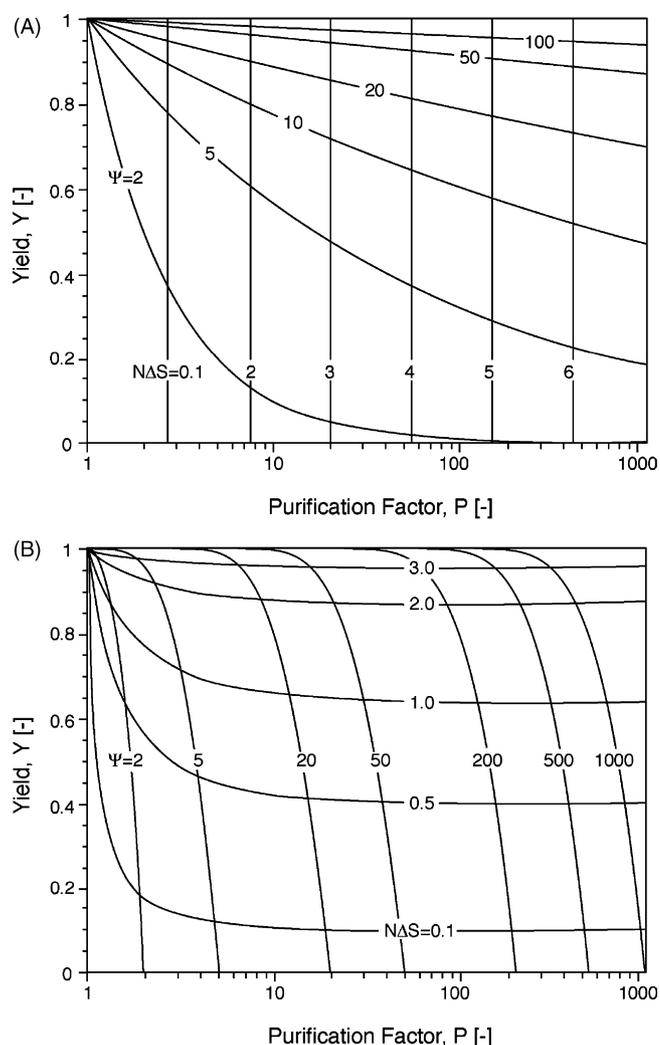
Fig. 28. (A) Optimization diagram for a retentate product showing trade-off between yield and purification factor as a function of selectivity $= S_{impurity}/S_{product}$ and mass throughput $= N\Delta S$ where $N = JAt/V$ with $J =$ filtrate flux, $A =$ membrane area, $t =$ diafiltration time, and $V =$ retentate volume. From van Reis and Saksena [79]. (B) Optimization diagram for a filtrate product showing trade-off between yield and purification factor as a function of selectivity $= S_{impurity}/S_{product}$ and mass throughput $= N\Delta S$ where $N = JAt/V$ with $J =$ filtrate flux, $A =$ membrane area, $t =$ diafiltration time, and $V =$ retentate volume. From van Reis and Saksena [79].

and for a product collected in the permeate:

$$P_p = \frac{Y_p}{1 - (1 - Y_p)^{1/\psi}} = \frac{Y_p}{1 + (Y_p - 1)\exp(N\,\Delta S)} \qquad (17)$$

The selectivity (ψ) is defined as the ratio of the sieving coefficient for the impurity to that of the product. The throughput is equal to the number of diavolumes (N) multiplied by the difference in the sieving coefficients for the impurity and product (ΔS). Fig. 28A and B show optimization diagrams, with the product yield plotted as a function of the purification factor for different values of the selectivity and throughput.

9.5.3.2. Operating parameters. HPTFF is optimized by measuring product and impurity sieving coefficients as a function of flux. The selectivity (ψ) and throughput parameter ($N\Delta S$)

Table 3
Monoclonal antibody product purity for an affinity process using Protein-A resin, cation exchange resin (bind/elute mode), anion exchange resin (flow-through mode), and ultrafiltration/diafiltration and a non-affinity based process using cation exchange resin, anion exchange resin, and HPTFF

Analyte	Affinity process	HPTFF process
Host cell proteins	<1 ppm	<1 ppm
DNA	<0.003 ppm	<0.006 ppm
MAb monomer	99.8%	99.5%

Data obtained by Bénédicte Lebreton and Robert van Reis at Genentech, Inc.

can then be plotted as a function of transmembrane pressure, with the best trade-off between selectivity and throughput then determined using the optimization equations or diagrams.

Several other parameters will also influence the selectivity and throughput. Buffer pH, conductivity, and ionic species play a critical role. In general, higher conductivities will shield charges on proteins and reduce the selectivity. This may be less important when separating monomer and multimers or other species with similar net charge.

The following guidelines apply to HPTFF separations in which the product is in the retentate and the impurities are in the filtrate. Buffer pH values distant from the product p*I* will reduce product sieving and enhance yields. Buffer pH values close to the p*I* of the impurity will enhance sieving and improve purity. A pH between the product and impurity p*I* values (and generally closer to the impurity p*I*) will typically give the best results. If multiple impurities are present it may also be advantageous to use either a step or continuous pH gradient during diafiltration. When the impurity p*I* values are less than the product p*I*, the pH gradient should generally be run from low to high pH so that impurities are always either positively charged or neutral before being removed thereby avoiding the potential for binding impurities to the positively charged membrane.

Membrane pore size and ligand density are also key parameters. A good starting point is to use a pore size of 100 kDa for antigen binding fragments (Fab) and 300 kDa for monoclonal antibodies. Increased ligand density will generally increase the buffer conductivity that can be used while maintaining product retention and enhancing impurity removal. Fig. 29 shows a non-reduced SDS-PAGE gel comparing the performance of a non-affinity monoclonal antibody purification process using an HPTFF step with that of a process using Protein A affinity chromatography for the bulk of the purification. The final product pools have nearly identical product profiles and impurity levels (Table 3), demonstrating the capability of using HPTFF for protein purification.

Buffer species play a key role in selectivity and throughput. Monovalent buffer ions are generally preferred since multivalent ions may bind to both proteins and membranes thereby reducing the net charge on both. For specific applications, however, this can leveraged as an advantage. It is also possible to first retain the product of interest with a monovalent buffer species (such as acetate) while removing lower molecular weight impurities (for example host cell proteins) and then switch to a multivalent buffer species (such as citrate) and enable the product to be transported through the membrane while retaining larger molecular
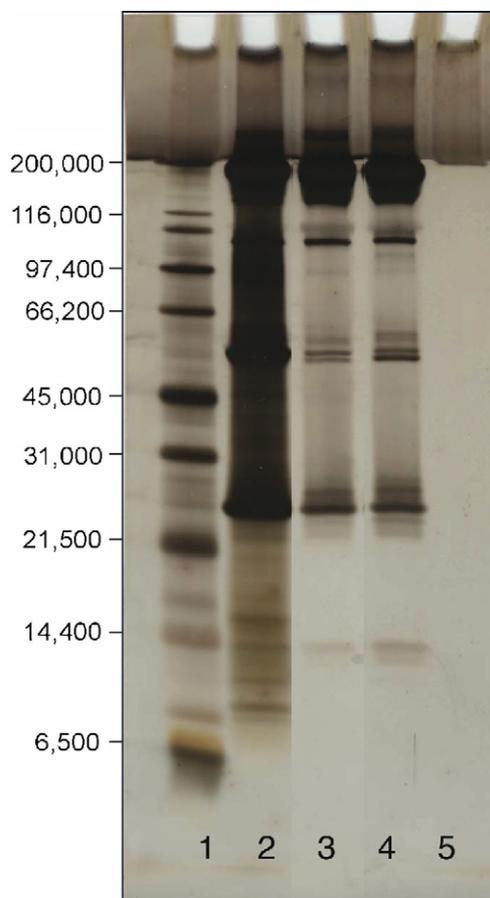
Fig. 29. Non-reduced SDS-PAGE gel comparing performance of non-affinity and protein-A affinity purification processes for a monoclonal antibody. All bands in the final pools are product-related as determined by mass spectrometry. Lane 1: Molecular weight standards, 2: Harvested cell culture fluid, 3: bulk purified by cation exchange chromatography, anion exchange chromatography, and HPTFF, 4: bulk purified by protein-A affinity chromatography, cation exchange chromatography, anion exchange chromatography, and ultrafiltration/diafiltration. Results from Bénédicte Lebreton and Robert van Reis at Genentech, Inc.

weight impurities (such as viruses, DNA, product multimers, and larger host cell proteins). Various non-ionic additives can also be used to enhance the separation without affecting the buffer conductivity.

The protein concentration during HPTFF diafiltration should be optimized for selectivity, throughput, and operating parameters (see Section 8.5). The feed flow rate can also be varied. If experiments are performed with co-current filtrate flow, the results without co-flow can be estimated by integrating over the length of the device based on curves showing selectivity and throughput as a function of TMP using the known TMP profile for the same device when operated without co-current filtrate flow.

10. Membrane characterization

10.1. Integrity tests

Integrity testing is critical for all membrane filters to insure that the system operates at the required level of performance. This is particularly true for critical unit operations like virus removal and sterile filtration. A number of non-destructive integrity tests have been developed based on the displacement of a fluid from the pores by a second fluid (or gas), with the rate of displacement providing a measure of the membrane retention characteristics and/or the presence of large defects.

10.1.1. Bubble point

The bubble point is determined by measuring the gas flow rate through a fully wetted membrane at progressively increasing levels of pressure [80]. The bubble point is defined as the pressure at which the liquid filled pore is first intruded by a gas. In small modules, the bubble point can be observed by a vigorous stream of bubbles exiting the membrane on the filtrate side. For large modules, the bubble point is typically identified by an inflection in the flow rate versus pressure curve indicative of liquid displacement from the largest pores. Bubble point measurements are primarily used for microfiltration membranes, which typically have bubble points in the 0.2×10^5–8×10^5 Pa (0.2–8 bar) range for 0.65–0.1 μm pore sizes using water as the wetting fluid.

10.1.2. Gas diffusion

Air diffusion measurements (also known as the forward flow test) are performed at a single pressure that is typically chosen at approximately 80% of the expected bubble point pressure (based on the maximum pore size or the size of the defects of greatest interest). The air flow rate through the wetted membrane is measured using an inverted graduated cylinder or an appropriate flow meter. Flow rates that exceed the manufacturer's specifications indicate the presence of defects that are large enough for the bubble point to be exceeded.

10.2. Porosimetry

Mercury porosimetry can be used to evaluate the pore volume distribution [81]. Mercury is a non-wetting fluid for most surfaces, thus the intrusion of mercury into the pores is a function of the applied pressure. The volume of intruded mercury at each pressure provides a measure of the volume distribution. Mercury porosimetry data can be difficult to interpret for membranes with significant pore throats since the volume behind the throat is measured at the intrusion pressure associated with the constricted diameter of the throat. In addition, the membranes must be characterized dry and mercury intrusion requires high pressures, both of which can alter the pore structure. Mercury porosimetry is most suitable for characterization of inorganic membranes with very stable structures.

10.3. Liquid–liquid integrity tests

Liquid–liquid integrity tests using fluids with very low interfacial tension can be used to identify the presence of defects that could not be identified using bubble point measurements since the required pressures would exceed the pressure ratings of the membrane and/or device [82]. The most common liquids are immiscible mixtures of alcohol and water or the two phases

produced by a mixture of ammonium sulfate, polyethylene glycol, and water. The flow rate of the intrusion fluid is evaluated at a specified transmembrane pressure for a membrane that has been thoroughly flushed with the wetting fluid. The module is then flushed with buffer, with the buffer flow rate evaluated at the same pressure. The CorrTest value (CTV) is defined as the logarithm (base 10) of the ratio of the buffer flow rate to the CorrTest fluid flow rate. CTV below a critical level are indicative of membrane failure.

10.4. Streaming potential

The streaming potential provides a measure of the membrane surface charge. Data can be obtained for flow along (tangential to) the membrane surface or for flow through the membrane pores. The streaming potential is defined as the voltage that develops to balance the net convective flux of counter-ions through the pores (or along the surface) of an electrically charged membrane. The voltage can be measured by Ag/AgCl electrodes as a function of the transmembrane pressure, with the slope of the resulting data used to evaluate the membrane zeta potential and surface charge density [83].

10.5. Dextran sieving

Ultrafiltration membranes are often characterized using either two proteins of different molecular weight (one retained and one passing solute) or using a mixture of dextrans covering a large molecular weight range. When using proteins it is important to note the pH and conductivity as these have a significant impact on the hydrodynamic volume and hence sieving of the proteins [15]. With both methods it is also important to note the mass transfer conditions. Stirred cells will typically have much lower mass transfer coefficients than tangential flow ultrafilters, which will impact the sieving performance [6]. Correlations have also been made between sieving of proteins, dextrans, and polyethylene glycols based on their Stokes radius [84].

The common mixed dextran test [85] uses a mixture of dextrans typically spanning a range of either 1–2000 kDa. Samples of feed and filtrate taken under steady-state conditions are run on size exclusion chromatography and the resulting filtrate chromatogram is divided by the feed chromatogram to provide sieving as a function of retention time. Retention time is converted to dextran molecular weight with a calibration curve generated by running individual dextran standards.

10.6. Flex test

Several enhancements to the mixed dextran test are incorporated into the so-called Flex Test [86]. The sensitivity of the test is increased by about 10-fold by using fluorescent tagged dextrans. While the conventional dextran test is typically used to specify a retention at $R = 0.9$ ("R90") or $S = 0.1$ (giving only 37% yield at $N = 10$ during a constant volume diafiltration), with a maximum sensitivity of $S = 0.01$ (90% yield at $N = 10$), the Flex Test can provide sieving measurements down to $S = 0.001$ (99% yield at $N = 10$). In addition the Flex Test has the option of
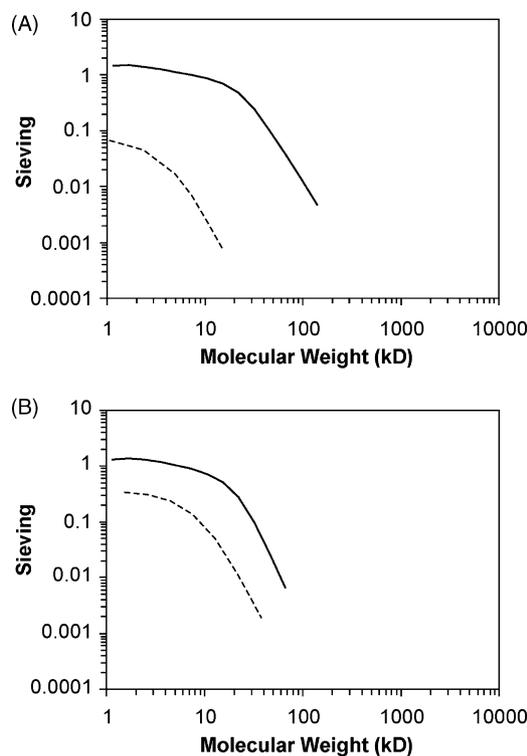
Fig. 30. Membrane characterization using the FlexTest employing fluorescently tagged and positively charged dextrans as highly retained solutes and neutral dextrans as passing solutes. Data obtained with a positively charged 300 kDa composite regenerated cellulose HPTFF membrane. Subpart (A) shows neutral dextrans (solid line) and fluorescent tagged positively charged dextrans (dotted line) on a 100 kDa positively charged composite regenerated cellulose membrane. Subpart (B) shows the same curves for a 300 kDa positively charged composite regenerated cellulose membrane. Adapted from Mulherkar and van Reis [86].

using fluorescent tagged charged dextrans to capture the effect of membrane charge on sieving. Chemical characteristics (charge and hydrophobicity) should be taken into account when selecting the fluorescent tag. For charged membranes, the sieving of a charged solute is usually measured with fluorescent tagged dextrans (high sensitivity for low sieving values) whereas the neutral dextrans may not require a fluorescent tag since they likely represent passing markers. The resolving power of different membranes can be compared by evaluating the selectivity and throughput parameters from data for the fluorescent charged and neutral dextrans. An example is provided in Fig. 30.

10.7. Leachables

Regulatory agencies require validated removal of leachables from filters used in the purification of human pharmaceuticals. Filter manufacturers determine the leachable content of their filters and perform safety testing in mice. Pharmaceutical manufacturers also need to validate the removal of filter leachables in the specific purification process. One method uses NMR to first generate a "fingerprint" of leachables from various solutions (low pH, high pH, and high conductivity) representative of the buffer conditions used in the purification process. Final bulks are then analyzed by NMR and compared against the filter

leachate spectra for identity. Acceptance criteria are usually less than 1–10 µg/mL.

11. System design

Both manual and automated filtration systems are commonly used throughout the biotechnology industry. The vast majority of systems in the biotechnology industry utilize batch processing. System design was originally based on equipment used in the food and dairy industries. A completely new set of designs has evolved to meet the more stringent requirements of the biotechnology industry. Systems with Steam-In-Place capability have been implemented where feasible (for example tangential flow microfiltration systems). Systems that employ membranes that cannot be steam sterilized have been re-designed to drastically improve bioburden control. Improved designs for components such as pumps, valves, and instruments have been implemented to meet requirements for low micro-cavitation (to reduce cell lysis and protein denaturation), low shear (to reduce cell lysis), and improved sanitary design. Novel control algorithms have also been implemented [69]. New components have been designed to handle the broad range of operating scales used in the biotechnology industry. Current systems use components that range in scale from 0.24 in. (6 mm) up to 6 in. (152 mm) diameter pipe sizes to enable processing at flow rates from 50 mL/min (process development, characterization and validation) up to 1400 L/min (industrial scale processing).

Ultrafiltration has become the unit operation of choice for concentration and formulation of final bulk protein products in the biotechnology industry [60]. The advent of high dose therapeutic antibodies has generated a requirement for ultrafiltration systems with very low operating hold-up volumes. High dose (100 mg) therapeutic proteins administered by subcutaneous injection (volume ≤ 1 mL) can be obtained by lyophilization followed by reconstitution using small diluent volumes. This often results in significant product losses when trying to recover a small volume from a large vial. The problem is accentuated by the high viscosity of many protein solutions at concentrations above 50 mg/mL. Product losses can be as high as 30% with a concomitant impact on plant capacity and cost of production. A second option is to use two ultrafiltration steps, one with sufficient area to formulate the product at an intermediate concentration (30–50 mg/mL) followed by a second smaller system used to carry out the final concentration up to 100–200 mg/mL. This option adds capital and operating costs to the product. The novel system design shown in Fig. 18 enables production of high concentration formulations in a single ultrafiltration step.

12. Future trends

Future trends in biotechnology will be driven by higher productivity, lower cost of production, and increased development speed. The first two goals can be accomplished by either reducing product doses (increased product specificity and/or efficacy) or by increasing cell culture titers, production scale, and purification productivity. There is also a trend toward increased use of disposable systems (bioreactors and buffer bags) and raw mate-

rials (single-use membranes) at pilot scale. As titers continue to increase, disposable systems may also become attractive for production scale manufacturing, eliminating the need for the development and validation of cleaning cycles.

As cell culture productivity increases there is typically an increase in cell debris load that must be removed during protein harvest. Positively charged cellulose depth filters are currently used in conjunction with either microfiltration or centrifugation for these purposes. Charged cellulose depth filtration is a very old technology that has proven to have unique characteristics for removal of wide particle size distribution debris and colloidal material. Improved chemical and physical characterization of harvest feed streams and improved understanding of removal mechanisms should be explored to improve harvest operations. Current depth filter cartridges are also very cumbersome to install and remove. Improved product design concepts should be developed to improve handling.

Significant progress has recently been made in developing high permeability and high capacity sterile filters. This has been accomplished with built-in pre-filters, composite membranes, pore size distribution gradients within individual membranes, improved chemistry, and increased membrane packing densities. Single-use sterile filters account for a significant part of raw materials cost in downstream processing. Steaming, cool-down, wetting, and integrity testing provide ongoing challenges for end-users. It is therefore desirable to develop more cost effective sterile filters with simple and robust operational characteristics.

Membrane chromatography has been evolving for some time without major utilization in the biotechnology industry. Low binding capacity has been one of the major obstacles. The ability to run at very high linear velocity has not offset the lower binding capacity since this leads to very large numbers of cycles per batch (about 100 versus 1 for resins) and equal requirements for re-use (100 runs for both media) to be cost effective. To be competitive for applications in which the product is bound, membranes will need to have equivalent binding capacity (>100 mg/mL for monoclonal antibodies), comparable media packing density ($\geq$60%), and similar process time and cost. Yield and purity already appear to be equivalent (see Section 7). The benefit of membranes would primarily be the elimination of packing and unpacking of media, which is a significant issue for manufacturing operations, especially at very large industrial scale (1000 L columns). If costs can be driven down sufficiently there may also be an opportunity for single use membrane chromatography units that would eliminate the need for some chromatography solutions (post-use sanitization and storage) thereby reducing capital and labor costs. Flow-through chromatography applications, in which the product flows through the matrix while low levels of impurities are bound, provide a more near-term application for membrane chromatography. High flow rate and low capacity media can be utilized for such applications and, unlike bind-and-elute applications, the economics are competitive for both re-use and single-use applications. Anion exchange membranes provide removal of viruses, DNA, and endotoxin comparable to resins [87]. Host cell proteins are, however, not cleared to the same extent without using lower conductivity buffers. This typically requires dilution, larger tanks, and larger

downstream unit operations. If host cell binding capacity could be made comparable to resins, single-use anion exchange membranes would be very attractive for manufacturing operations. Another application for membrane chromatography is for purification of very large solutes such as DNA, RNA, and viruses (used for example in gene therapy) that are too large to enter into the pores of conventional (bead-based) resins.

Virus retentive filters for protein feed streams have evolved from general large molecular weight cut-off ultrafiltration membranes to specially designed membrane structures capable of providing very high degrees of virus retention. Tangential flow mode has been replaced with normal flow operation and even small viruses (20 nm) can be separated from monoclonal antibodies with high clearance (5 log reduction) and high protein yields (>99%). Primary limitations of existing virus filters are relatively low permeability, low capacity, and high costs. Improved membrane structures and devices are needed to significantly reduce the size and cost of normal flow virus filtration.

Ultrafiltration (UF) has been used throughout downstream processing for concentration and diafiltration of products. Initial concentration and diafiltration of the harvested cell culture fluid has been largely eliminated due to the increase in titer of current feed streams and the availability of high flow rate resins with affinity ligands that operate without changing the pH and conductivity of the harvested cell culture fluid. Intermediate UF has

also been eliminated from many processes by matching elution buffers from one chromatography step with conditions required for subsequent steps or by using simple pH and conductivity adjustments. UF has, however, replaced size exclusion chromatography in almost all final formulation processes [60]. UF flux rates are in large part determined by the protein mass transfer coefficient, osmotic virial coefficients, and protein concentration at the membrane wall (surface). The mass transfer coefficient, virial coefficients, and wall concentration are intrinsic properties of the protein but vary with buffer pH and conductivity. Mass transfer is also determined by channel geometry (screen type) and feed flow rate. Systems have been developed to significantly increase mass transfer coefficients [30] but at the expense of membrane packing density. New ways of increasing mass transfer while maintaining high membrane packing density and low pressure drop provide one opportunity for improvement.

Commercial implementation of charged UF membranes provides another opportunity for improved fluxes, particularly for low molecular weight cut-off UF membranes (<10 kDa) (see Section 8). Charged UF membranes in conjunction with optimum operating parameters can also be used to enable protein purification with HPTFF (see Section 9). Composite regenerated cellulose membranes are low fouling (<20%), easy to clean (ambient 0.1N NaOH), and eliminate the physical weakness of conventional regenerated cellulose membranes. Further
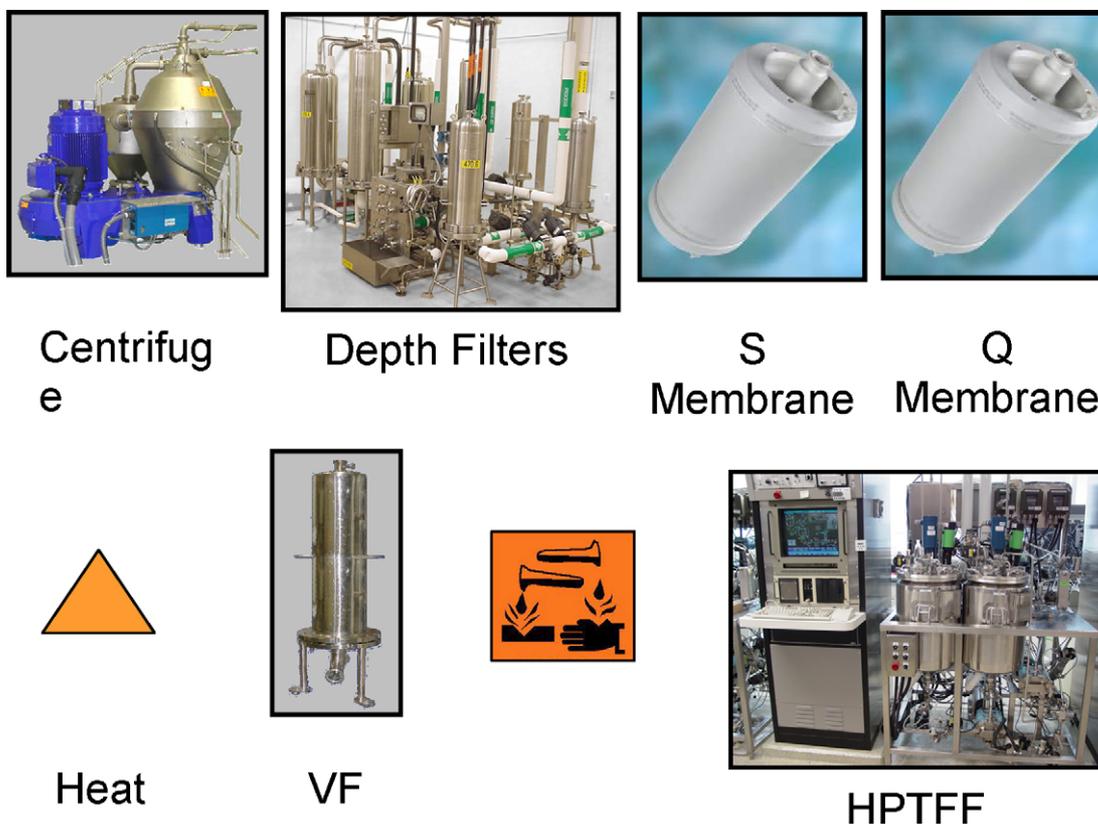
Fig. 31. Purification scheme for a monoclonal antibody using membrane technology. The monoclonal antibody is harvested by centrifugation (cell removal) and depth filtration (cell debris removal). The cation exchange membrane removes host cell proteins. The anion exchange membrane removes host cell protein, DNA, and any endotoxin and viruses. Heat, virus filtration, and acid treatment are used for virus inactivation and removal. High performance tangential flow filtration is used for antibody concentration, host cell protein removal, and buffer exchange (formulation). Process from Bénédicte Lebreton, Ai P. Lin, Nuno Fontes, Amit Mehta, and Robert van Reis at Genentech, Inc.

attempts to recreate these attributes with synthetic polymers will likely continue. Development of a family of UF membranes with optimum permeability should be pursued. Permeability values below about 5 L/m^2/h/psi become limiting relative to mass transfer and osmotic pressure, whereas permeability values above 20 L/m^2/h/psi cause significant gradients in filtrate flux along the length of the UF device without any improvement in the overall process flux due to mass transfer and osmotic pressure limitations. Disposable UF cartridges may emerge, although cost savings associated with the elimination of membrane cleaning must be traded off with increased labor for installation of cartridges on every run and the increased risk of installation integrity failures.

Membranes have traditionally been used to separate species of very different size such as proteins from cells (microporous/sterile filters), cell debris (depth filters), and viruses (virus filters), and for the separation of low molecular weight components from proteins (ultrafiltration). The development of membrane chromatography and HPTFF enable for the first time complete purification of proteins using membrane systems. Fig. 31 shows a process scheme for purification of a monoclonal antibody using a series of membrane-based unit operations. Although not implemented in any commercial processes, small-scale studies using this process show comparable yield, purification, and product quality with a conventional process. Future developments will determine whether such a membrane-based process can provide the required product quality, purity, yields, and throughput with reduced costs for the biotechnology industry.

Acknowledgments

References

[1] J.D. Ferry, Ultrafilter membranes and ultrafiltration, Chem. Rev. 18 (1936) 373.

[2] M.R. Ladisch, K.L. Kohlmann, Recombinant human insulin, Biotech. Progr. 8 (1992) 469.

[3] H.W. Blanch, D.S. Clark, Biochemical Engineering, Marcel Dekker, New York, 1997.

[4] F.V. Kosikowski, Membrane separations in food processing, in: W.C. McGregor (Ed.), Membrane Separations in Biotechnology, Marcel Dekker, Inc., New York, 1986.

[5] W.F. Blatt, A. Dravid, A.S. Michaels, L. Nelsen, Solute polarization and cake formation in membrane ultrafiltration. Causes, consequences, and control techniques, in: J.E. Flinn (Ed.), Membrane Science and Technology, Plenum Press, New York, 1970, pp. 47–97.

[6] L.J. Zeman, A.L. Zydney, Microfiltration and Ultrafiltration: Principles and Applications, Marcel Dekker, New York, 1996.

[7] R. van Reis, J.M. Brake, J. Charkoudian, D.B. Burns, A.L. Zydney, High performance tangential flow filtration using charged membranes, J. Membr. Sci. 159 (1999) 133.

[8] A. Mehta, A.L. Zydney, Effect of membrane charge on flow and protein transport during ultrafiltration, Biotech. Prog. 22 (2006) 484.

[9] R. van Reis, A.L. Zydney, Protein ultrafiltration, in: M.C. Flickinger, S.W. Drew (Eds.), Encyclopedia of Bioprocess Technology: Fermentation, Biocatalysis, and Bioseparation, John Wiley & Sons, Inc., New York, 1999, pp. 2197–2214.

[10] B. Hallstrom, M. Lopez-Leiva, Description of a rotating ultrafiltration module, Desalination 24 (1978) 273.

[11] K.Y. Chung, R. Bates, G. Belfort, Dean vortices with wall flux in a curved channel membrane system. 4. Effect of vortices on separation fluxes of suspensions in microporous membrane, J. Membr. Sci. 81 (1993) 139.

[12] J.M. Reichert, C.J. Rosensweig, L.B. Faden, M.C. Dewitz, Monoclonal antibody successes in the clinic, Nat. Biotech. 23 (2005) 1073.

[13] I. Gitlin, J.D. Carbeck, G.M. Whitesides, Why are proteins charged? Networks of charge-charge interactions in proteins measured by charge ladders and capillary electrophoresis, Angew. Chem. Int. Ed. 45 (2006) 3022.

[14] N.S. Pujar, A.L. Zydney, Electrostatic and electrokinetic interactions during protein transport through narrow pore membranes, Ind. Eng. Chem. Res. 33 (1994) 2473.

[15] N.S. Pujar, A.L. Zydney, Electrostatic effects on protein partitioning in size exclusion chromatography and membrane ultrafiltration, J. Chromatogr. A 796 (1998) 229.

[16] C.L. Keefer, Production of bioproducts through the use of transgenic animal models, Anim. Reprod. Sci. 82–83 (2004) 5.

[17] K. Ko, H. Koprowski, Plant biopharming of monoclonal antibodies, Virus Res. 111 (2005) 93.

[18] A.M. Voloshin, J.R. Swartz, Efficient and scalable method for scaling up cell free protein synthesis in batch mode, Biotech. Bioeng. 20 (2005) 516.

[19] M.A. Serabian, A.M. Pilaro, Safety assessment of biotechnology-derived pharmaceuticals: ICH and beyond, Toxicol. Pathol. 27 (1999) 27.

[20] A.S. Rosenberg, Effects of protein aggregates: an immunologic perspective, AAPS J. 8 (2006) 501.

[21] H.A. Doyle, M.J. Mamula, Post-translational protein modifications in antigen recognition and autoimmunity, Trends Immunol. 22 (2001) 443.

[22] J. Hermia, Constant pressure blocking filtration laws—application to power-law non-newtonian fluids, Trans. Inst. Chem. Eng.-Lond. 60 (1982) 183.

[23] C.-C. Ho, A.L. Zydney, A combined pore blockage and cake filtration model for protein fouling during microfiltration, J. Colloid Interface Sci. 232 (2000) 389.

[24] C.-C. Ho, A.L. Zydney, Protein fouling of asymmetric and composite microfiltration membranes, Ind. Eng. Chem. Res. 40 (2001) 1412.

[25] A.L. Zydney, C.-C. Ho, Effect of membrane morphology on system capacity during normal flow microfiltration, Biotech. Bioeng. 83 (2003) 537.

[26] F. Badmington, M. Payne, R. Wilkins, E. Honig, V$_{max}$ testing for practical microfiltration train scale-up in biopharmaceutical processing, Pharmaceut. Tech. 19 (1995) 64.

[27] Health Industry Manufacturers Association (HIMA), Microbiological Evaluation of Filters for Sterilizing Liquids, HIMA Document No. 3, vol. 4, 1982.

[28] S. Sundaram, M. Auriemma, G. Howard, H. Brandwein, F. Leo, Application of membrane filtration for removal of diminutive bioburden organisms in pharmaceutical products and processes, PDA J. Pharm. Sci. Tech. 53 (1999) 186.

[29] R. van Reis, L.C. Leonard, H.C. Chung, S.E. Builder, Industrial scale harvest of proteins from mammalian cell culture by tangential flow filtration, Biotech. Bioeng. 38 (1991) 413.

[30] G. Belfort, R.H. Davis, A.L. Zydney, The behavior of suspensions and macromolecular solutions in crossflow microfiltration, J. Membr. Sci. 96 (1994) 1.

[31] A.L. Zydney, C.K. Colton, A concentration polarization model for filtrate flux in cross-flow microfiltration of particulate suspensions, Chem. Eng. Commun. 47 (1986) 1.

[32] R.W. Field, D. Wu, J.A. Howell, B.B. Gupta, Critical flux concept for microfiltration fouling, J. Membr. Sci. 100 (1995) 259.

[33] A. Pollice, A. Brookes, B. Jefferson, S. Judd, Sub-critical flux fouling in membrane bioreactons—a review of recent literature, Desalination 174 (2005) 221.

[34] B.D. Cho, A.G. Fane, Fouling transients in nominally sub-critical flux operation of a membrane bioreactor, J. Membr. Sci. 209 (2002) 391.

[35] R. Singhvi, C. Schorr, C. O'Hara, L. Xie, D.I.C. Wang, Clarification of animal cell culture process fluids using depth microfiltration, BioPharm. (1996) 35.

[36] Y. Yigzaw, R. Piper, M. Tran, A.A. Shukla, Exploitation of the adsorptive properties of depth filters for host cell protein removal during monoclonal antibody purification, Biotech. Prog. 22 (2006) 288.

[37] R.W. Waterson, Novel depth filtration technologies: strategies for process development, Pharmaceut. Eng. 10 (1990) 22.

[38] H.R. Charlton, J.M. Relton, N.K.H. Slater, Characterisation of a generic monoclonal antibody harvesting system for adsorption of DNA by depth filters and various membranes, Bioseparation 8 (1999) 281.

[39] E.A. Ostreicher, R.A. Knight, J.V. Fiore, E. Southington, K.C. Hou, Charge modified microporous membrane, process for charge modifying said membrane and process for filtration of fluid, US Pat No. 4473474:1 (1984).

[40] K. Brorson, L. Norling, E. Hamilton, S. Lute, K. Lee, S. Curtis, Y. Xu, Current and future approaches to ensure the viral safety of biopharmaceuticals, Dev. Biol. (Basel) 118 (2004) 17.

[41] T. Burnouf, M. Radosevich, Nanofiltration of plasma-derived biopharmaceutical products, Haemophilia 9 (2003) 24.

[42] J. Carter, H. Lutz, An overview of viral filtration in biopharmaceutical manufacturing, Eur. J. Parenteral Sci. 7 (3) (2002) 72.

[43] A.J. DiLeo, A.E. Allegrezza, S.E. Builder, High resolution removal of virus from protein solutions using a membrane of unique structure, Bio/Technology 10 (1992) 182.

[44] H. Brough, C. Antoniou, J. Carter, J. Jakubik, Y. Xu, H. Lutz, Performance of a novel Viresolve NFR virus filter, Biotech. Prog. 18 (2002) 782.

[45] G.R. Bolton, S. Spector, D. Lacasse, Increasing the capacity of parvovirus-retentive membranes: performance of the Viresolve prefilter, Biotechnol. Appl. Biochem. 43 (2006) 55.

[46] K.H. Oshima, T.T. Evans-Strickfaden, A.K. Highsmith, E.W. Ades, The use of a microporous polyvinylidene fluoride (PVDF) membrane filter to separate contaminating viral particles from biologically important proteins, Biologicals 24 (1996) 137.

[47] N.M. Troccoli, J. McIver, A. Losikoff, J. Poiley, Removal of viruses from human intravenous immune globulin by 35 nm nanofiltration, Biologicals 26 (1998) 321.

[48] T. Tsurumi, T. Sato, N. Osawa, H. Hitaka, T. Hirasaki, K. Yamaguchi, Y. Hamamoto, T. Manabe, T. Yamashiki, N. Yamamoto, Structure and filtration performances of improved caprammonium regenerated cellulose hollow fiber (improved BMM hollow fiber) for virus removal, Polym. J. 22 (12) (1990) 1085–1100.

[49] A. Johnston, A. MacGregor, S. Borovec, M. Hattarki, K. Stuckly, D. Anderson, N.H. Goss, A. Oates, E. Uren, Inactivation and clearance of viruses during the manufacture of high purity factor IX, Biologicals 28 (2000) 129.

[50] R.W. van Holten, S.M. Autenrieth, Evaluation of depth filtration to remove prion challenge from an immunoglobulin preparation, Vox. Sang. 85 (2003) 20.

[51] T. Hongo-Hirasaki, K. Yamaguchi, K. Yanagida, K. Okuyama, Removal of small viruses (parvovirus) from IgG solution by virus removal filter Planova®20N, J. Membr. Sci. 278 (2006) 3.

[52] G.R. Bolton, M. Cabatingan, M. Rubino, S. Lute, K. Brorson, M. Bailey, Normal-flow virus filtration: detection and assessment of the endpoint in bio-processing, Biotechnol. Appl. Biochem. 42 (2005) 133.

[53] J.X. Zhou, T. Tressel, Basic concepts in q membrane chromatography for large-scale antibody production, Biotech. Prog. 22 (2006) 341.

[54] S.Y. Suen, M.R. Etzel, Sorption kinetics and breakthrough curves for pepsin and chymosin using pepstatin A affinity membranes, J. Chromatogr. A 686 (1994) 179.

[55] C. Harinarayan, J. Mueller, A. Junglof, R. Fahrner, J. van Alstine, R. van Reis, An exclusion mechanism in ion exchange chromatography, Biotech. Bioeng. (2006).

[56] X. Zeng, E. Ruckenstein, Membrane chromatography: preparation and applications to protein separation, Biotech. Prog. 15 (1999) 1003.

[57] H.L. Knudsen, R.L. Fahrner, Y. Xu, L.A. Norling, G.S. Blank, Membrane ion-exchange chromatography for process-scale antibody purification, J. Chromatogr. A 907 (2001) 145.

[58] H.N. Endres, J.A. Johnson, C.A. Ross, J.K. Welp, M.R. Etzel, Evaluation of an ion-exchange membrane for the purification of plasmid DNA, Biotechnol. Appl. Biochem. 37 (2003) 259.

[59] M.A. Teeters, S.E. Conrardy, B.L. Thomas, T.W. Root, E.N. Lightfoot, Adsorptive membrane chromatography for purification of plasmid DNA, J. Chromatogr. A 989 (2003) 165.

[60] R.T. Kurnik, A.W. Yu, G.S. Blank, A.R. Burton, D. Smith, A.M. Athalye, R. van Reis, Buffer exchange using size exclusion chromatography, countercurrent dialysis, and tangential flow filtration: models, development, and industrial application, Biotech. Bioeng. 45 (1995) 149.

[61] A. Mehta, A.L. Zydney, Permeability and selectivity analysis for ultrafiltration membranes, J. Membr. Sci. 249 (2005) 245.

[62] V. Vilker, C. Colton, K. Smith, The osmotic pressure of concentrated protein solutions: effect of concentration and pH in saline solutions of bovine serum albumin, J. Colloid Interface Sci. 79 (1981) 548.

[63] G. Gehlert, S. Luque, G. Belfort, Comparison of ultra- and microfiltration in the presence and absence of secondary flow with polysaccharides, proteins, and yeast suspensions, Biotech. Prog. 14 (1998) 931.

[64] R. van Reis, E.M. Goodrich, C.L. Yson, L.N. Frautschy, S. Dzengeleski, H. Lutz, Linear scale ultrafiltration, Biotech. Bioeng. 55 (1997) 737.

[65] A.R. Da Costa, A.G. Fane, D.E. Wiley, Spacer characterization and pressure drop modeling in spacer-filled channels for ultrafiltration, J. Membr. Sci. 87 (1994) 79.

[66] J. Schwinge, D.E. Wiley, A.G. Fane, Novel spacer design improves observed flux, J. Membr. Sci. 229 (2004) 53.

[67] P. Ng, J. Lundblad, G. Mitra, Optimization of solute separation by diafiltration, Sep. Sci. 2 (1976) 499.

[68] J.H. Shao, A.L. Zydney, Optimization of ultrafiltration/diafiltration processes for partially bound impurities, Biotech. Bioeng. 87 (2004) 286.

[69] R. van Reis, E.M. Goodrich, C.L. Yson, L.N. Frautschy, R. Whiteley, A.L. Zydney, Constant Cwall ultrafiltration process control, J. Membr. Sci. 130 (1997) 123.

[70] A.L. Zydney, Stagnant film model for concentration polarization in membrane systems, J. Membr. Sci. 23 (1997) 275.

[71] V.L. Vilker, C.K. Colton, K.A. Smith, Concentration polarization in protein ultrafiltration. 1. An optical shadowgraph technique for measuring concentration profiles near a solution-membrane interface, AIChE J. 27 (1981) 632.

[72] J.C. Chen, Q. Li, M. Elimelech, In situ monitoring techniques for concentration polarization and fouling phenomena in membrane filtration, Adv. Coll. Interface Sci. 107 (2004) 83.

[73] R. van Reis, S. Gadam, L.N. Frautschy, S. Orlando, E.M. Goodrich, S. Saksena, R. Kuriyel, C.M. Simpson, S. Pearl, A.L. Zydney, High performance tangential flow filtration, Biotech. Bioeng. 56 (1997) 71.

[74] A.L. Zydney, R. van Reis, High performance tangential flow filtration, in: W.K. Wang (Ed.), Membrane Separations in Biotechnology, second ed., Marcel Dekker, New York, 2001, pp. 277–298.

[75] M.F. Ebersold, A.L. Zydney, Separation of protein charge variants by ultrafiltration, Biotech. Prog. 20 (2004) 543–549.

[76] R. van Reis, Tangential flow filtration process and apparatus, U.S. Patents 5,256,294 (1993) and 5,490,937 (1996).

[77] S. Saksena, A.L. Zydney, Effect of solution pH and ionic strength on the separation of albumin from immunoglobulins (IgG) by selective membrane filtration, Biotech. Bioeng. 43 (1994) 960.

[78] B. Cheang, A.L. Zydney, A two-stage ultrafiltration process for fractionation of whey protein isolate, J. Membr. Sci. 231 (2004) 159.

[79] R. van Reis, S. Saksena, Optimization diagram for membrane separations, J. Membr. Sci. 129 (1997) 19.

[80] S. Emory, Principles of integrity testing hydrophilic microporous membranes, Pharm. Technol. 13 (1989) 68.

[81] F.P. Cuperus, C.A. Smolders, Characterization of UF membranes, Adv. Colloid Interface Sci. 34 (1991) 135.

[82] M.W. Phillips, A.J. DiLeo, A validatible porosimetric technique for verifying the integrity of virus-retentive membranes, Biologicals 24 (1996) 243.

[83] D.B. Burns, A.L. Zydney, Effect of solution pH on protein transport through semipermeable ultrafiltration membranes, Biotech. Bioeng. 64 (1999) 27.

[84] L.J. Zeman, M. Wales, Steric rejection of polymeric solutes by membranes with uniform pore size distribution, Sep. Sci. Technol. 16 (3) (1981) 275–290.

[85] G. Tkacik, S. Michaels, A rejection profile test for ultrafiltration membranes and devices, Bio/Technology 9 (1991) 941.

[86] P. Mulherkar, R. van Reis, Flex test: a fluorescent dextran test for UF membrane characterization, J. Membr. Sci. 236 (2004) 171.

[87] M. Phillips, J. Cormier, J. Ferrence, C. Dowd, R. Kiss, H. Lutz, J. Carter, Performance of a membrane adsorber for trace impurity removal in biotechnology manufacturing, J. Chromatogr. A 1078 (2005) 74–82.